

The Effects of Diaphragm Components in Resisting Lateral Stability of Precast Concrete Frames

Vot 75139

LAPORAN AKHIR

6 November 2006

Research Leader: Assoc. Prof. Dr. Ahmad Baharuddin Abd. Rahman
Faculty of Civil Engineering, UTM Skudai

ABSTRACT

Frame system structures which composed of only reinforced concrete columns, beams and slabs, have been recently adopted for many framed buildings. Generally, flexural stiffness of slabs is ignored in the conventional analysis of bare frame structures. However, in reality, the floor slabs may have some influence on the lateral response of the structures. Consequently, if the flexural stiffness of slabs in a frame system structure is totally ignored, the lateral stiffness of the global frames may be underestimated. Therefore, the objective of the research is to investigate the effects of floor diaphragms in multi-storey frames by comparing the two models of frames with slabs and without slabs. The results show that the slabs can slightly increase the lateral stability of bare frames by about 10% to 18%. Furthermore, it can be seen from the study that the main important role of the slab is actually to act as a deep beam in transferring the horizontal loads from the slabs to the columns.

ABSTRAKS

Pada masa kini, sistem kerangka konkrit bertertulang yang terdiri daripada tiang, rasuk dan papak telah digunakan dalam industri pembinaan bangunan tinggi. Perisian COSMOS/M ialah satu perisian yang biasanya dipakai untuk menjalankan analisis terhadap bangunan tinggi dan analisis tersebut adalah berdasarkan kepada konsep analisis unsur terhingga tak lelelus (NLFEA). Walaubagaimanapun, papak mungkin akan mempengaruhi kelakuan ufuk bagi sesuatu struktur. Jika kekukuhan lenturan pada papak diabaikan, kemungkinan kekukuhan ufuk bagi keseluruhan bangunan akan dianggarkan kurang dari sepatutnya. Dengan ini, tujuan kajian ini adalah untuk mengkaji kesan-kesan papak dalam sistem kerangka yang bertingkat. Perbandingan anantara sistem kerangka yang berpapak dan sistem kerangka yang tidak berpapak telah dilakukan dalam kajian ini untuk mendapatkan kesan-kesannya.

TABLE OF CONTENTS

CHAPTER	TITLE	PAGE
	TITLE	i
	DECLARATION	ii
	DEDICATON	iii
	ACKNOWLEDGEMENT	iv
	ABSTRACT	v
	ABSTRAK	vi
	TABLE OF CONTENTS	vii
	LITST OF TABLES	xi
	LIST OF FIGURES	xii
	LIST OF SYMBOLS	xv
	LIST OF APPENDICES	xvi
CHAPTER 1	INTRODUCTION	1
	1.1 General Introduction	1
	1.2 Statement of the Problem	2
	1.3 Aims and Objectives of the Present Study	3
	1.4 Scope of Study	3

CHAPTER 2	LITERATURE REVIEW	4
2.1	Introduction	4
2.2	Structural Concepts	5
2.3	Structural Form	12
2.3.1	Braced-frame Structures	12
2.3.2	Infilled-Frame Structures	14
2.3.3	Flat-Plate and Flat-Slab Structures	15
2.4	Floor System	16
2.4.1	One-Way Slabs on Beams or Walls	16
2.4.2	One-Way Slab on Beams and Girders	17
2.4.3	Two-Way Slab and Beam	18
2.5	Material Properties for Concrete	18
2.5.1	Stress-Strain Relationship for Concrete	19
2.6	Finite Element Analysis	20
2.6.1	Non-linear Finite Element Analysis (NLFEA)	21
2.6.2	Finite Element Modelling	23
2.6.3	Computer Program for the Finite Element Analysis	24
CHAPTER 3	MODELLING OF THE DIAPHRAGMS AND THREE DIMENSIONAL FRAME	25
3.1	Introduction	25
3.2	COSMOS/S Software	26
3.3	COSMOS/M Method	27
3.4	Finite Element Modelling	28
3.4.1	Element Shape	28
3.4.2	Frame Geometry	30
3.4.3	Material Properties	32
3.4.4	Material Curve for Concrete	33

3.4.5	Meshing	36
3.4.6	Boundary Condition and Loading	38
3.4.7	Solution Procedures	40
3.4.7.1	Arc Length Control	40
3.4.7.2	Iterative Solution Method	41
3.4.7.3	Termination Criteria	43
3.4.8	Results	45
3.5	Conclusion	45
CHAPTER 4	VERIFICATION OF FINITE ELEMENT MODEL	46
4.1	Introduction	46
4.2	Description of the Model	47
4.3	Comparison of Deformed Shapes Of the Floor Diaphragms	47
4.4	Load-Deflection Characteristics of the Frame Structure	49
4.5	Conclusion	50
CHAPTER 5	LINEAR BEHAVIOUR OF FLOOR DIAPHRAGM	51
5.1	Introduction	51
5.2	Load-Deflection Characteristics of the Frame Structure	52
5.3	Output of Stress Analysis of the Frame Structure	53
5.3.1	Von Mises Stress	53
5.3.2	In Plane Shear Stress	54
5.3.3	Diaphragm Action	56
5.4	Conclusion	58

CHAPTER 6	NON-LINEAR BEHAVIOUR OF FLOOR DIAPHRAGMS	59
6.1	Introduction	59
6.2	Nonlinear Finite Element Analysis	60
6.2.1	Load-Deflection Characteristics of the Frame Structure	60
6.2.2	Behaviour of Stress Analysis of the Frame Structure	62
6.2.2.1	Concrete Cracking	63
6.2.2.2	Concrete Crushing	67
6.3	Conclusion	69
CHAPTER 7	CONCLUSIONS AND RECOMMENDATIONS	70
7.1	Introduction	70
7.2	Conclusions	70
7.3	Recommendations for Future Research Work	71
REFERENCE		73
APPENDICES		76
Appendix A–B		76-79

LIST OF TABLES

TABLE NO.	TITLE	PAGE
3.1	Limitation of entities in COSMOS/M	26
3.2	Geometrical entities for the model	31
3.3	Input data for nonlinear solution control	44
5.1	Comparison of frame deflections	53
6.1	Comparison of frame deflections	60

LIST OF FIGURES

FIGURE NO.	TITLE	PAGE
2.1	Structural concept of tall building	6
2.2	Buildings shear resistance: (a) Building must not break; (b) Building must not deflect excessively in shear	6
2.3	Bending resistance of building: (a) Building must not overturn; (b) Columns must not fail in tension or compression; (c) Bending deflection must not be excessive	7
2.4	Building plan forms: (a) Uniform distribution of columns; (b) Columns concentrated at the edges	8
2.5	Column layout and Bending Rigidity Index (BRI): (a) Square building with corner columns: BRI=100; (b) Traditional building of the 1930s, BRI=33; (c) Modern tube building, BRI=33; (d) Sears Towers, BRI=33; (e) City Corp Tower: BRI=33; (f) Building with corner and core columns, BRI=56; (g) Bank of Southwest Tower, BRI=63	9
2.6	Tall building shear systems: (a) Shear wall system; (b) Diagonal web system; (c) Web system with diagonals and horizontals	11
2.7	Rigid frame	13
2.8	Infilled frame	14
2.9	One-way slab	17
2.10	One-way slab on beams and girders	17
2.11	Two-way slab and beam	18

2.12	Typical stress-strain curve for concrete	19
2.13	Short-term stress-strain curves for concrete of different cube strengths	20
3.1	Analysis Steps using COSMOS/M	27
3.2	COSMOS/M menu related to PT, CR, SF and VL	28
3.3	Description of the 3D Isoparametric Solid Element	29
3.4	Frame structure geometry model by COSMOS/M	30
3.5	Plan view of the structures with a rigid slab diaphragm	31
3.6	Plan Dimension	31
3.7	Stress-strain curve for concrete	33
3.8	Stress-strain curve for concrete (Adopted from Marsono, 2000)	34
3.9	COSMOS/M menu related to the input of stress-strain data	34
3.10	COSMOS/M menu for meshing	36
3.11	3D view of the model after meshing	37
3.12	(a) Side view; (b) Front view and (c) Plan view	38
3.13	Loadings and restraints of model; (a) 3D view and (b) Side view	39
3.14	COSMOS/M menu which shows the Arc-length method	41
3.15	COSMOS/M menu which shows the NR method	42
3.16	Modified Newton-Raphson Method	43
3.17	COSMOS/M menu for NL_CONTROL command	44
3.18	COSMOS/M menu for checking the available result	45
4.1	Loadings and restraints of model; (a) 3D view and (b) Side view	47
4.2	Comparison of the deformed shape for the slabs: (a) Result from Dong-Guen Lee, (b) Result from COSMOS/M (3D view), (c) Result from COSMOS/M (side view)	48
4.3	Comparison of the deformed shape for the global frame model: (a) Result from COSMOS/M; (b) Result from Dong-Guen Lee (2002)	49
4.4	Comparison of displacement results between COSMOS/M and Dong-Guen Lee(2002)	50
5.1	Deflection curve for frame structure under constant loading	52
5.2	Contour plot of the Von Mises stress in 3D and plan view	54
5.3	Contour plot of the in plane shear stress of frame structure with slabs	55
5.4	Contour plot of the in plane shear stress of frame structure without slabs	56

5.5	Actions in a diaphragm (Strut and Tie Model)	57
6.1	Load-deflection curve	61
6.2	Deformed shape of frame structure; (a) 3D view and (b) Side view	62
6.3	Contour plot of maximum principal stress, P_1 , at arc step 17	64
6.4	Contour plot of deflection at arc step 17	65
6.5	Contour plot of maximum principal stress, P_1 , at arc step 19	66
6.6	Contour plot of deflection at arc step 19	67
6.7	Contour plot of the minimum principal stress, P_3 , of the frame structure model which include slabs (Arc step 77)	68
6.8	Contour plot of the minimum principal stress, P_3 , of the frame structure model which excluding slabs (Arc step 83)	69

LIST OF SYMBOLS

E	-	Modulus of Elasticity
f_{cu}	-	Concrete compression strength
f_{max}	-	Concrete maximum stress
f_t	-	Concrete tensile strength
f_y	-	Steel tensile strength
ε	-	Strain
ε_{co}	-	Compressive strain in concrete at maximum compressive stress
ε_{cr}	-	Tensile strain in concrete at maximum tensile stress
ε_{cu}	-	Concrete ultimate strain
μ	-	Poisson's ratio
σ	-	Stress

LIST OF APPENDICES

APPENDIX	TITLE	PAGE
A	Stress-Strain Data for Concrete in Compression	76
B	SES File for Frame Model in COSMOS/M	78

CHAPTER 1

INTRODUCTION

1.1 General Introduction

Tall towers and buildings have fascinated mankind from the beginning of civilization, their construction being initially for defense and subsequently for ecclesiastical purpose. The growth in modern tall building construction, however, which began in the 1880s, has been largely for commercial and residential purpose.

Tall commercial buildings are primarily a response to the demand by business activities to be as close to each other, and to the city center, as possible, thereby putting intense pressure on the available land space. Also, because they form distinctive landmarks, tall commercial buildings are frequently developed in city centers as prestige symbols for corporate organizations. Further, the business and tourist community, with its increasing mobility, has fuelled a need for more, frequently high-rise, city center hotel accommodations.

The rapid growth of the urban population and the consequent pressure on limited space has considerably influenced city residential development. The high cost

of land, the desire to avoid a continuous urban sprawl, and the need to preserve important agricultural production have all contributed to drive residential buildings upward. In some cities, for example, Hong Kong and Rio de Janeiro, local topographical restrictions make tall buildings the only feasible solution for housing needs.

1.2 Statement Of The Problem

In conventional design, usually the slabs of a whole floor are ignored in the analysis of frame. Thus, the flexural stiffness of slabs is usually not included in the analysis of frame. This assumption may be reasonable for bare framed structure. However, the floor slabs may have a significant influence on the lateral response of structures. If the flexural stiffness of slab in the frame system is totally ignored, the lateral stiffness of the structures may be significantly underestimated. In order to predict accurate lateral load response of a frame system structures, it may be prudent to include an appropriate amount of flexural stiffness of slabs.

Hence the statement of problem in this study is to find out the relationship between lateral stiffness and lateral deflection of frames based on flexural stiffness of slabs.

1.3 Aims and Objectives of the Present Study

With the development of high-speed personal computers nowadays, numerical methods have been widely used in solving engineering non-linear problems. Therefore, the main objectives of this study are: -

- To analyze the effects of floor slabs for high-rise building structures.
- To study the effect of slabs to the lateral stiffness of the building.
- To study the transfer of horizontal shear forces in the floor diaphragms.

1.4 Scope of Study

The present study is focused on the behaviour of the effects of floor slabs in the frame due to lateral loading and the transfer of the shear forces in the slab diaphragms. The study will bring out the non-linear finite element analysis for the frame to obtain the softening point, which is the ultimate failure load of the frame.

The study is limited to the following scopes:

- Only reinforced concrete framed structures are considered.
- The frame considered is a 2 x 3 bays with 10 storeys height.
- The frame is subjected to static incremental lateral loads.

CHAPTER 2

LITERATURE REVIEW

2.1 Introduction

In the '60s and early '70s, the evolution of new structural form for tall buildings gave stimulus to the development of method of analysis. Much of the research has been done, and approximate analytical methods are available for almost all the identifiable regular forms of high-rise structure. More powerful and sophisticated computer programs for general structural analysis are now widely available, as well as some comprehensive programs for tall building analysis. Consequently the designer is usually able to analyse the most complex high-rise structure without recourse to the researcher.

From the structural engineer's point of view, the determination of the structural form of a high-rise building would ideally involve only the selection and arrangement of the major structural elements to resist most efficiently the various combinations of gravity and horizontal loading. In reality, however, the choice of structural form is usually strongly influenced by other than structural considerations. The range of factors that has to be taken into account in deciding the structural form includes the internal planning, the material and method of construction, the external

architectural treatment, the planned location and routing of the service systems, the nature and magnitude of the horizontal loading, and the height and proportions of the building. The taller and more slender a building, the more important the structural factors become, and the more necessary it is to choose an appropriate structural form.

2.2 Structural Concepts

The key idea in conceptualising the structural system for a narrow tall building is to think of it as a beam cantilevering from the earth (Fig. 2.1). The laterally directed force generated, either due to wind blowing against the building or due to the inertia forces induced by ground shaking, tends both to snap it (shear), and push it over (bending). Therefore, the building must have a system to resist shear as well as bending. In resisting shear forces, the building must not break by shearing off (Fig. 2.2a), and must not strain beyond the limit of elastic recovery (Fig. 2.2b). Similarly, the system resisting the bending must satisfy three needs (Fig. 2.3). The building must not overturn from the combined forces of gravity and lateral loads due to wind or seismic effects; it must not break by premature failure of columns either by crushing or by excessive tensile forces; its bending deflection should not exceed the limit of elastic recovery. In addition, a building in seismically active regions must be able to resist realistic earthquake forces without losing its vertical load carrying capacity.

In the structure's resistance to bending and shear, a tug-of-war ensues that sets the building in motion, thus creating a third engineering problem; motion perception or vibration. If the building sways too much, human comfort is sacrificed, or more importantly, non-structural elements may break resulting in expensive damage to the building contents and causing danger to the pedestrians.

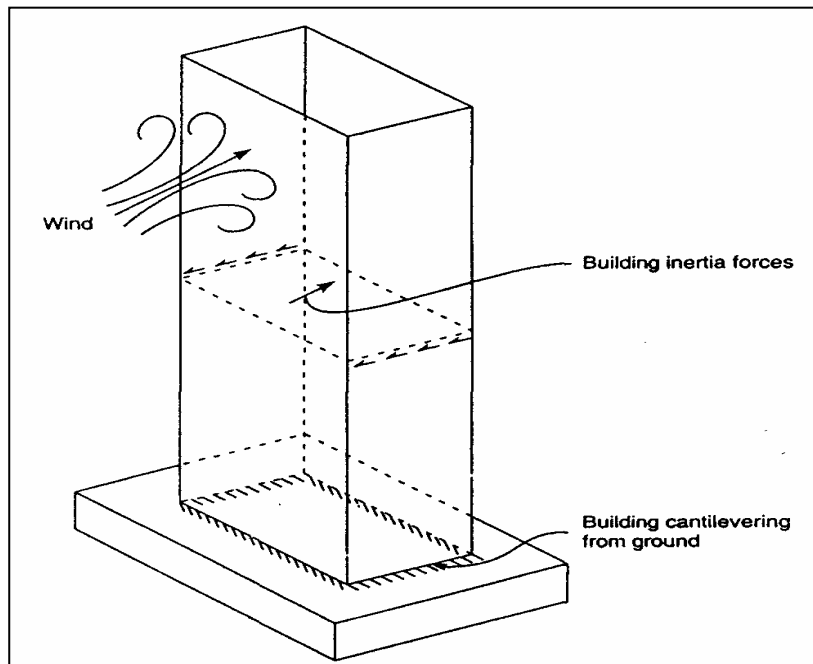


Figure 2.1: Structural concept of tall building (Bungale S. Taranath, 1988)

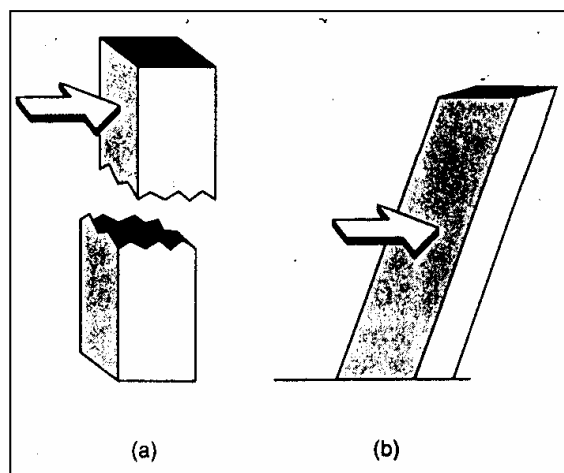


Figure 2.2: Buildings shear resistance: (a) Building must not break; (b) Building must not deflect excessively in shear (Bungale S. Taranath, 1988)

A perfect structural form to resist the effects of bending, shear and excessive vibration is a system possessing vertical continuity ideally located at the farthest extremity from geometric center of the building. A concrete chimney is perhaps an ideal, if not an inspiring engineering model for a rational super-tall structural form. The quest for the best solution lies in translating the ideal form of the chimney into a more practical skeletal structure.

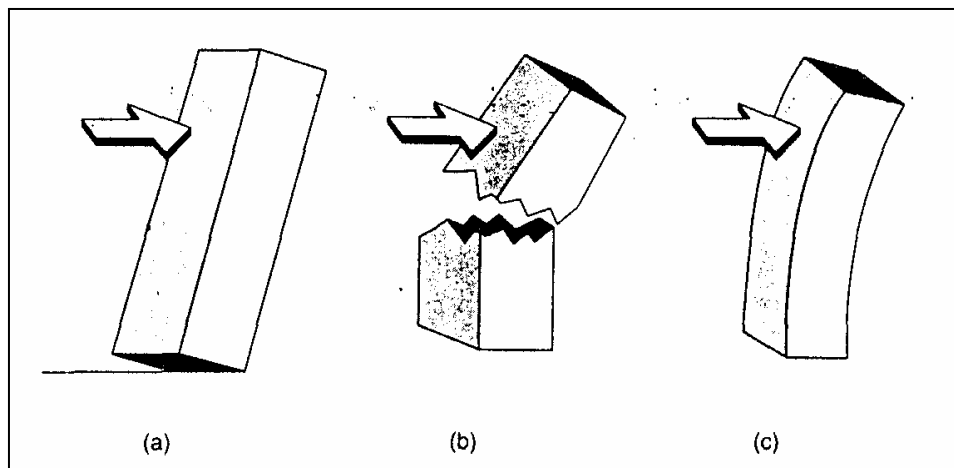


Figure 2.3: Bending resistance of building: (a) Building must not overturn; (b) Columns must not fail in tension or compression; (c) Bending deflection must not be excessive (Bungale S. Taranath, 1988)

With the proviso that a tall building is a beam cantilevering from earth, it is evident that all columns should be at the edges of the plan. Thus the plan shown in Fig. 2.4(b) would be preferred over the plan in Fig. 2.4(a). Since this arrangement is not always possible, it is of interest to study how the resistance to bending is affected by the arrangement of columns in plan. We will use two parameters, Bending Rigidity Index (BRI) and Shear Rigidity Index (SRI), first published in *Progressive Architecture*, to explain the efficiency of structural systems.

The ultimate possible bending efficiency would be manifest in a square building which concentrates all the building columns into four corner columns as shown in Fig. 2.5(a). Since this plan has maximum efficiency it is assigned the ideal Bending Rigidity Index (BRI) of 100. The BRI is the total moment of inertia of all the building columns about the centroidal axes participating as an integrated system.

The traditional tall building of the past, such as the Empire State Building, used all columns as part of the lateral resisting system. For columns arranged with regular bays, the BRI is 33 (Fig. 2.5b).

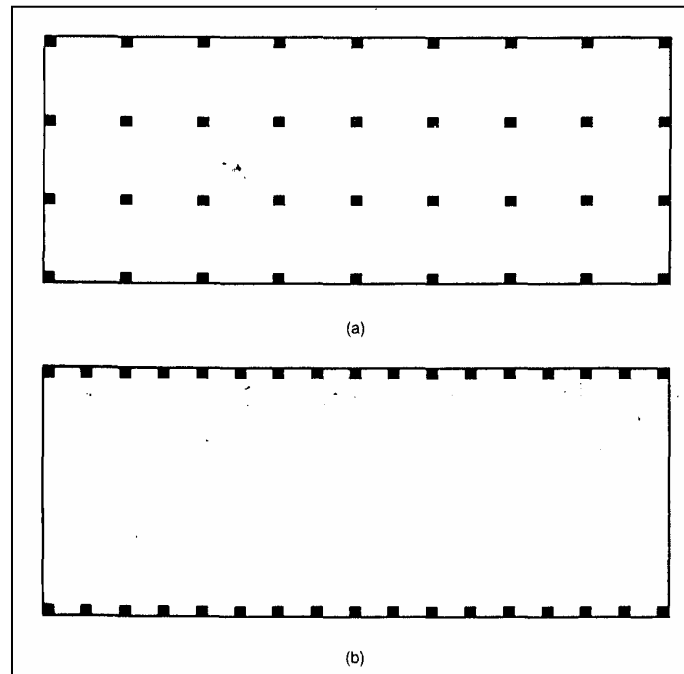


Figure 2.4: Building plan forms: (a) Uniform distribution of columns; (b) Columns concentrated at the edges (Bungale S. Taranath, 1988)

A modern tall building of the 1980s and 90s has closely spaced exterior columns and long clear spans to the elevator core in an arrangement called “tube”. If only the perimeter columns are used to resist the lateral loads, the BRI is 33. An example of this plan type is the World Trade Center in New York City (Fig. 2.5c).

The Sear Towers in Chicago uses all its columns as part of the lateral system in a configuration called a “bundled tube”. It also has a BRI of 33 (Fig. 2.5d).

The Citicorp Tower (Fig. 2.5e) uses all of its columns as part of its lateral system, but because columns could not be placed in the corners, its BRI is reduced to 31. If the columns were moved to the corners, the BRI would be increased to 56

(Fig. 2.5f). Because there are eight columns in the core supporting the loads, the BRI falls short of 100.

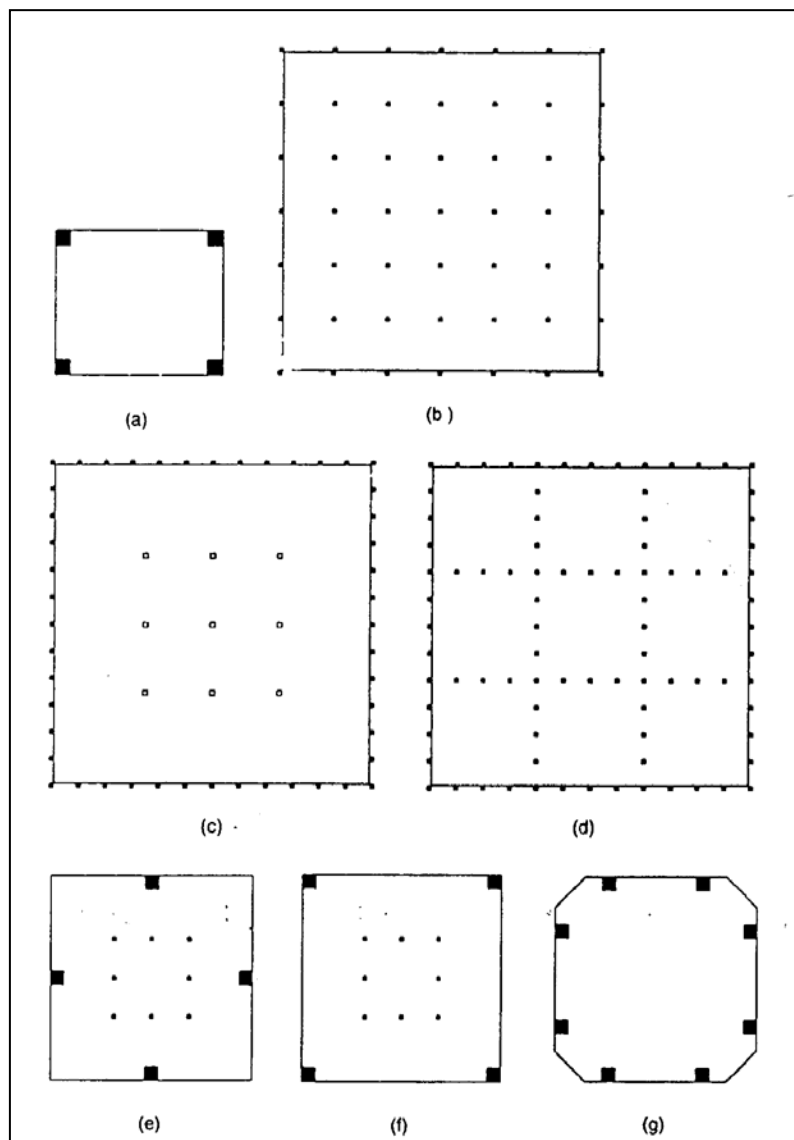


Figure 2.5: Column layout and Bending Rigidity Index (BRI): (a) Square building with corner columns: BRI=100; (b) Traditional building of the 1930s, BRI=33; (c) Modern tube building, BRI=33; (d) Sears Towers, BRI=33; (e) City Corp Tower: BRI=33; (f) Building with corner and core columns, BRI=56; (g) Bank of Southwest Tower, BRI=63, (Bungale S. Taranath,1988)

The plan of Bank of Southwest Tower, a proposed tall building in Houston, Texas, approaches the realistic ideal for bending rigidity with a BRI of 63 (Fig. 2.5g). The corner columns are split and displaced from the corners to allow generous views from office interiors.

In order for the columns to work as elements of an integrated system, it is necessary to interconnect them with an effective shear-resisting system. Let us look at some of the possible solutions and their relative Shear Rigidity Index (SRI). The ideal shear system is a plate or wall without openings which has an ultimate Shear Rigidity Index (SRI) of 100 (Fig. 2.6a). The second-best shear system is a diagonal web system at 45 degree angles which has an SRI of 62.5 (Fig. 2.6b). A more typical bracing system which combines diagonals and horizontals but uses more material is shown in Fig. 2.6c. Its SRI depends on the slope of the diagonals and has a value of 31.3 for the most usual brace angle of 45 degrees.

The most common shear systems are rigidly joined frames as shown in Fig. 2.6d-g. The efficiency of a frame as measured by its SRI depends on the proportions of members' lengths and depths. A frame, with closely spaced columns, like those shown in Fig. 2.6e-g, used in all four faces of a square building has a high shear rigidity and doubles up as an efficient bending configuration. The resulting configuration is called a "tube" and is the basis of innumerable tall buildings including the world's two most famous buildings, the Sears Tower and the World Trade Center.

In designing the lateral bracing system for buildings it is important to distinguish between a "wind design" and "seismic design". The building must be designed for horizontal forces generated by wind or seismic loads, whichever is greater, as prescribed by the building code or site-specific study accepted by the Building Official. However, since the actual seismic forces, when they occur, are likely to be significantly larger than code-prescribed forces, seismic design requires material limitations and detailing requirements in addition to strength requirements.

Therefore, for buildings in high-seismic zones, even when wind forces govern the design, the detailing and proportioning requirements of seismic resistance must also be satisfied. The requirements get progressively more stringent as the zone factor for seismic risk gets progressively higher.

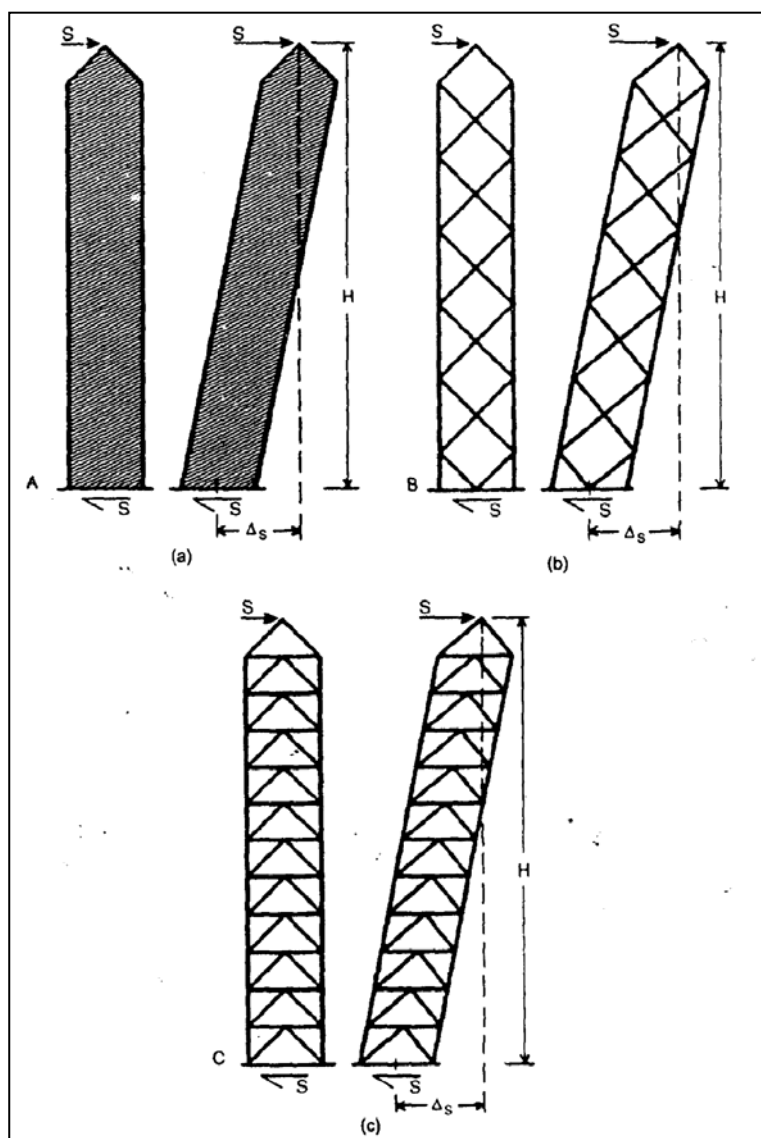


Figure 2.6: Tall building shear systems: (a) Shear wall system; (b) Diagonal web system; (c) Web system with diagonals and horizontals (Bungale S. Taranath, 1988)

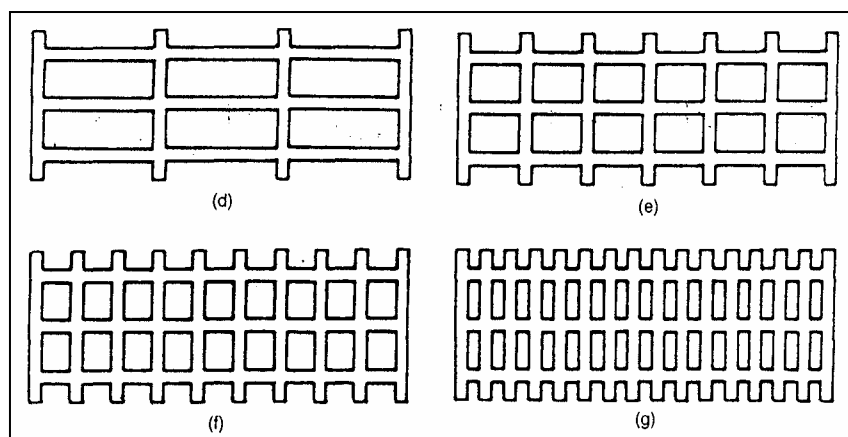


Figure 2.6 (continued): (d-g) Rigid frames (Bungale S. Taranath, 1988)

2.3 Structural Form

2.3.1 Rigid-Frame Structures

Rigid-frame structures consist of columns and girders joined by moment-resistant connections. The lateral stiffness of a rigid-frame bent depends on the bending stiffness of columns, girders, and connections in the plane of the bent (Fig. 2.7). The rigid frame's principal advantage is its open rectangular arrangement, which allows freedom of planning and easy fitting of doors and windows. If used as the only source of lateral resistance in a building, in its typical 20 ft (6m) - 30 ft (9m) bay size, rigid framing is economic only for buildings up to about 25 stories. Above 25 stories the relatively high lateral flexibility of the frame calls for uneconomically large members in order to control the drift.

Rigid-frame construction is ideally suited for reinforced concrete buildings because of the inherent rigidity of reinforced concrete joints. The rigid-frame form is also used for steel frame buildings, but moment-resistant connections in steel tend to be costly. The sizes of the columns and girders at any level of a rigid frame are

directly influenced by the magnitude of the external shear at that level, and they therefore increase toward the base. Consequently, the design of the floor framing cannot be repetitive as it is in some braced frames. A further result is that sometimes it is not possible in the lowest stories to accommodate the required depth of girder within the normal ceiling space.

Gravity loading also is resisted by the rigid-frame action. Negative moments are induced in the girders adjacent to the columns causing the mid-span positive moments to be significantly less than in a simply supported span. In structures in which gravity loads dictate the design, economies in member sizes that arise from this effect tend to be offset by the higher cost of the rigid joints.

While rigid frames of a typical scale that serve alone to resist lateral loading have an economic height limit of about 25 stories, smaller scale rigid frames in the form of perimeter tube, or typically scaled rigid frames in combination with shear walls or braced bents, can be economic up to much greater heights.

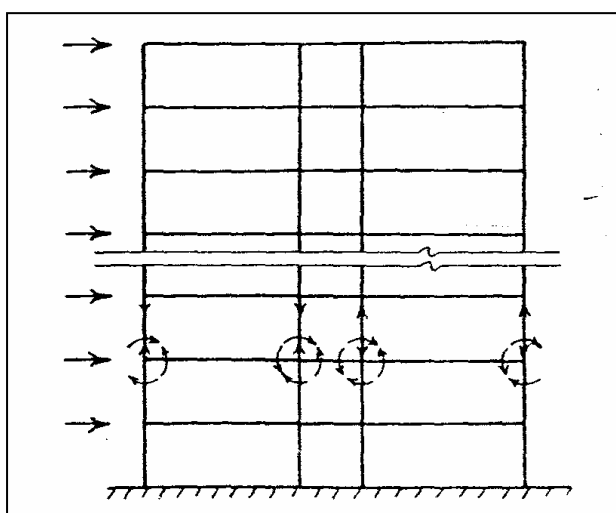


Figure 2.7: Rigid frame (Bryan Stafford Smith, 1991)

2.3.2 Infilled-Frame Structures

In many countries infilled frames are the most usual form of construction for tall buildings of up to 30 stories in height. Column and girder framing of reinforced concrete, or sometimes steel, is infilled by panels of brickwork, block work, or cast-in-place concrete.

When an infilled frame is subjected to lateral loading, the infill behaves effectively as a strut along its compression diagonal to brace the frame (Fig. 2.8). Because the infills serve also as external walls or internal partitions, the system is an economical way of stiffening and strengthening the structure.

The complex interactive behaviour of the infill in the frame, and the rather random quality of masonry, has made it difficult to predict with accuracy the stiffness and strength of an infilled frame. Indeed, at the time of writing, no method of analysing infilled frames for their design has gained general acceptance. For these reasons, and because of the fear of the unwitting removal of bracing infills at some time in the life of the building, the use of the infills for bracing tall buildings has mainly been supplementary to the rigid-frame action of concrete frames.

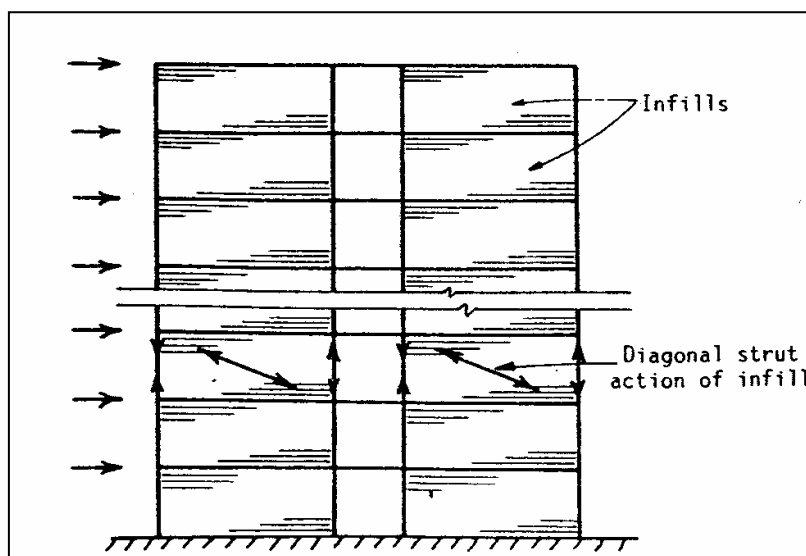


Figure 2.8: Infilled frame (Bryan Stafford Smith, 1991)

2.3.3 Flat-Plate and Flat-Slab Structures

The flat-plate structure is the simplest and most logical of all structural forms in that it consists of uniform slabs, of 5-8 in. (12-20 cm) thickness, connected rigidly to supporting columns. The system, which is essentially of reinforced concrete, is very economical in having a flat soffit requiring the most uncomplicated formwork and, because the soffit can be used as the ceiling, in creating a minimum possible floor depth.

Under lateral loading the behaviour of a flat-plate structure is similar to that of a rigid frame, that is, its lateral resistance depends on the flexural stiffness of the components and their connections, with the slabs corresponding to the girders of the rigid frame. It is particularly appropriate for apartment and hotel construction where ceiling spaces are not required and where the slab may serve directly as the ceiling. The flat-plate structure is economical for spans of up to about 25 ft (8 m), above which drop panels can be added to create a flat-slab structure for span of up to 38 ft (12 m).

Buildings that depend entirely for their lateral resistance on flat-plate or flat-slab action are economical up to about 25 stories. Previously, however, when Code requirements for wind design were less stringent, many flat-plate buildings were constructed in excess of 40 stories, and are still performing satisfactorily.

2.4 Floor System

An appropriate floor system is an important factor in the overall economy of the building. Some of the factors that influence the choice of the floor system are architectural. For example, in residential buildings, where smaller permanent divisions of the floor space are required, shorter floor span are possible; whereas, in modern office buildings, that require more open, temporarily sub divisible floor spaces, longer span systems are necessary. Other factors affecting the choice of floor system are related to its intended structural performance, such as whether it is to participate in the lateral load-resisting system, and to its construction, for example, whether there is urgency in the speed of erection.

Reinforced concrete floor systems are grouped into two categories; one-way, in which the slab spans in one direction between supporting beams or walls, and two-way, in which the slab spans in orthogonal directions. In both systems, advantage is taken of continuity over interior supports by providing negative moment reinforcement in the slab.

2.4.1 One-Way Slabs On Beams Or Walls

A solid slab of up to 8 in. (0.2m) thick, spanning continuously over walls or beams up to 24 ft (7.4m) apart (Fig. 2.9), provides a floor system requiring simple formwork, possibly flying formwork, with simple reinforcement. The system is heavy and inefficient in its use of both concrete and reinforcement. It is appropriate for use in cross-wall and cross-frame residential high-rise construction and, when constructed in a number of uninterrupted continuous spans, lends itself to prestressing.

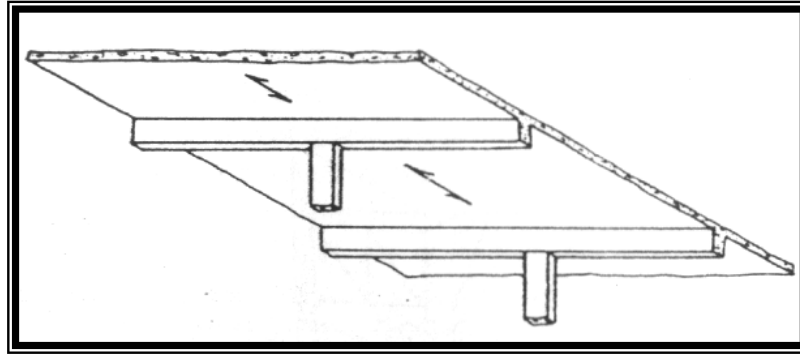


Figure 2.9: One-way slab (Bryan Stafford Smith, 1991)

2.4.2 One-Way Slab on Beams and Girders

A one-way slab spans between beams at a relatively close spacing while the beams are supported by girders that transfer the load to the columns (fig. 2.10). The short spanning slab may be thin, from 3 to 6 in. (7.6-15 cm) thick, while the system is capable of providing long spans of up to 46 ft (14 m). The principal merits of the system are its long span capability and its compatibility with a two-way lateral load resisting rigid-frame structure.

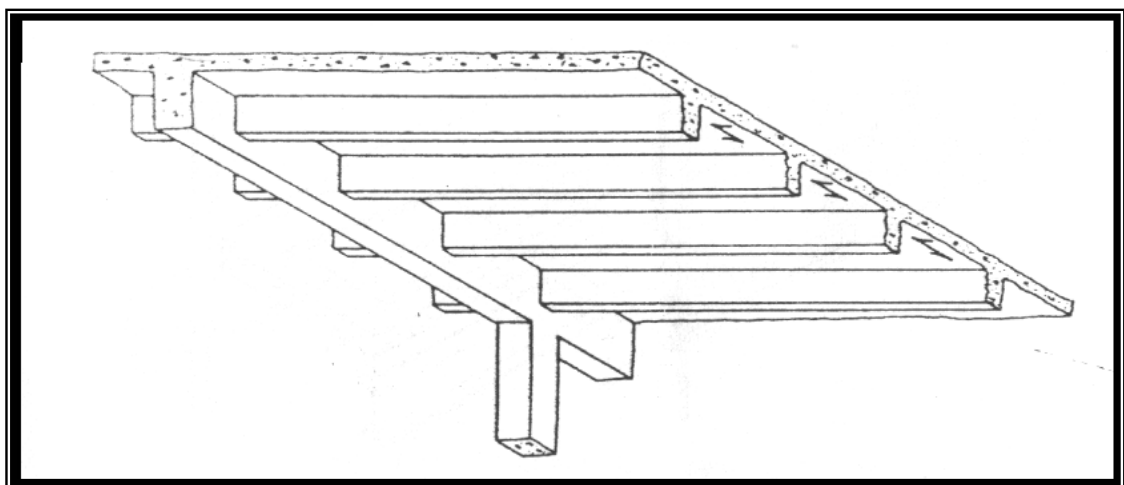


Figure 2.10: One-way slab on beams and girders (Bryan Stafford Smith, 1991)

2.4.3 Two-Way Slab and Beam

The slab spans two ways between orthogonal sets of beams that transfer the load to the columns or walls (Fig. 2.11). The two-way system allows a thinner slab and is economical in concrete and reinforcement. It is also compatible with a lateral load-resisting rigid-frame structure. The maximum length-to-width ratio for a slab to be effective in two directions is approximately 2.

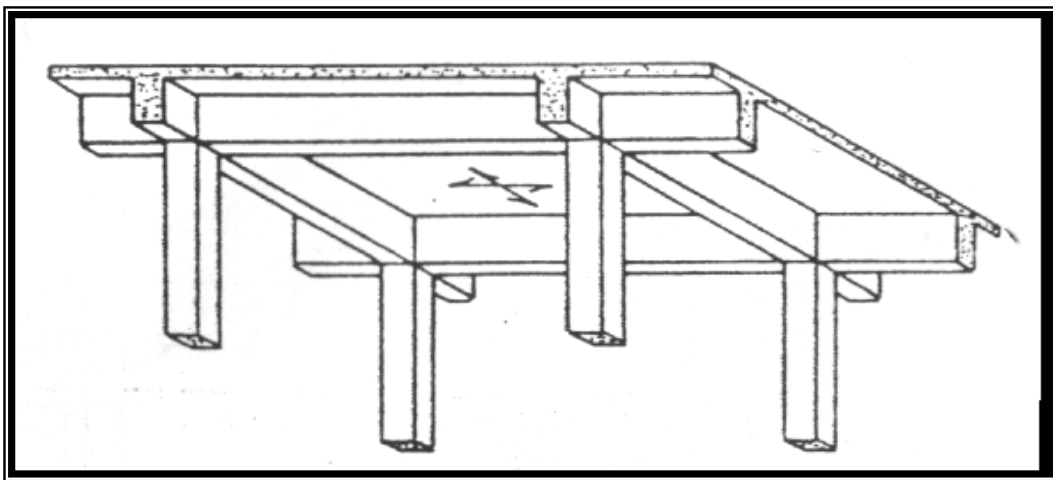


Figure 2.11: Two-way slab and beam (Bryan Stafford Smith, 1991)

2.5 Material Properties for Concrete

A clear understanding of the way in which the component material, concrete, react to applied load is an essential preliminary to full analysis of an element. One of the important properties is the stress-strain relationship.

2.5.1 Stress-Strain Relationship for Concrete

Figure 2.12 shows the typical idealized stress-strain curve for concrete. The properties of concrete are harder to predict in comparison to steel due to the complex nature of the concrete properties itself. The strain at any instant in concrete is composed of a mixture of elastic and plastic effects, dependent not only on the previous loading history but also on (to mention but some of the many possible causes of strain in the material) such diverse factors as the ambient conditions, the relative thickness of the concrete and its composition (Knowles, 1973).

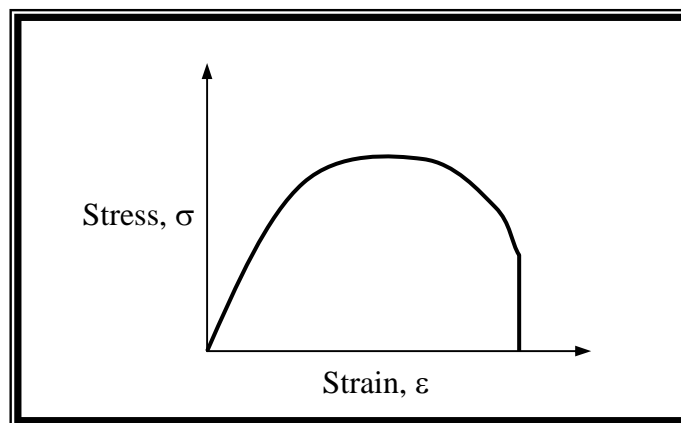


Figure 2.12: Typical stress-strain curve for concrete (Knowles, 1973)

Typical short-term stress-strain curves for three different concrete with compressive strengths of 20, 40 and 60 N/mm² are shown in Figure 2.13. From the figure, concrete stress may be assumed proportional to strain, provided that the appropriate modulus of elasticity being used and value of stresses do not exceed about 0.4 N/mm² of the compressive strength of the concrete. This statement is only applicable for elastic design.

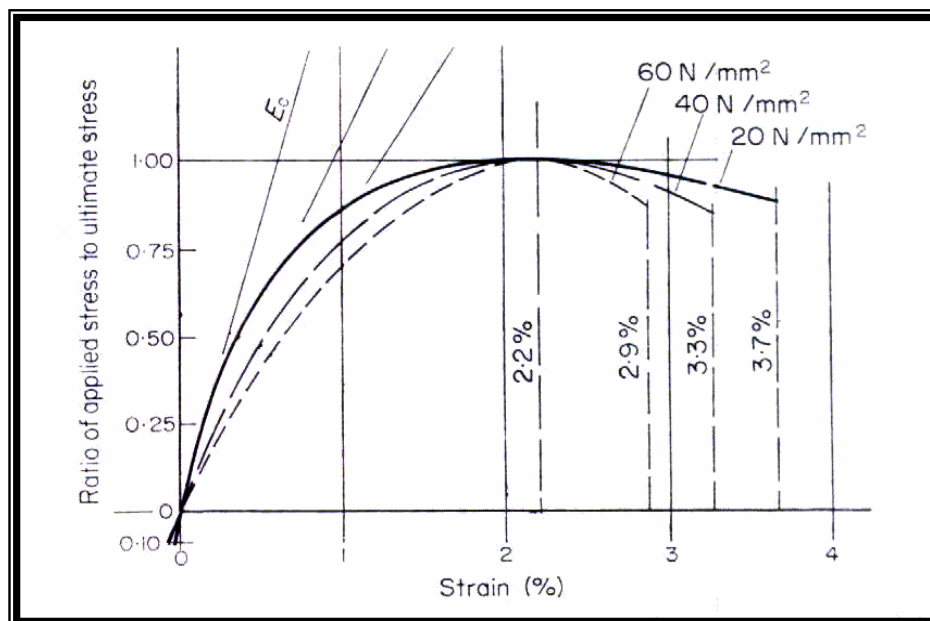


Figure 2.13: Short-term stress-strain curves for concrete of different cube strengths (Knowles, 1973)

2.6 Finite Element Analysis

Finite element is a sub region of a discretized continuum. It is of finite size (not infinitesimal) and usually has a simpler geometry than that of the continuum. The finite-element method enables us to convert a problem with an infinite number of degrees of freedom to one with a finite number in order to simplify the solution process. Although the original applications were in the area of solid mechanics, its usage has spread to many other fields having similar mathematical bases. In any case it is a computer-oriented method that must be implemented with appropriate digital computer programs. The primary objectives of analysis by finite element are to calculate approximately the stresses and deflections in a structure.

The classical approach for analysing a solid requires finding a stress or displacement function that satisfies the differential equations of equilibrium, the stress-strain relationship, and the compatibility conditions at every point in the continuum, including the boundaries. Because these requirements are so restrictive, very few classical solutions have been found. Among those, the solutions are often infinite series that in practical calculations require truncation, leading to approximate results. Furthermore, discretization of the differential equations by the method of finite differences has the primary disadvantage that boundary conditions are difficult to satisfy. The secondary disadvantage is that accuracy of the results is usually poor. On the other hand, the finite element approach yields an approximate analysis based upon an assumed displacement field, a stress field, or mixture of these within each element.

2.6.1 Non-linear Finite Element Analysis (NLFEA)

Non-linear finite element techniques have been used successfully to model many types of elements in a concrete structure. The theory of non-linear states that when an external force acting on a deformable element, it will experience deformation and resulting in internal forces. Nonlinearity is introduced by the non-linear form of the constitutive relationships for concrete in compression and by concrete tensile cracking, as well as by the variable contact area with the ground support. Generally, non-linear analysis will only applicable to three conditions as stated below:

1. Any material in the state of static
2. Any material in the state of kinematics
3. Any material which comply to the Hooke's Law

More recently, NLFEA or non-linear finite element analysis applications to reinforced concrete structures have improved remarkably due to research and advances in computer technology. NLFEA is ready to become a sufficiently practical tool for researching, designing, maintaining, and upgrading common constructed facilities. The application of NLFEA is in great demand as the analysis method involves visualisation of the user and the result is much easier to interpret and understand.

It is very important to conduct a linear analysis to understand the behaviour of the model before conducting a non-linear analysis. Certain important parameters can be obtained from studying the linear modelling. (Huria, *et. al*, 1993). The NLFEA using softwares available in market should be tested and verified thoroughly against experimental data before full confidence can be put on the reliability of the software (Marsono and Subedi, 2000).

One of the most important aspects of finite element modelling is the mesh design. Strain gradients across first order elements are linear, which means if the mesh used is too coarse then complex areas of the structure are not modelled accurately. If the mesh size is too small, however, the number of constraints within the model will increase, this reduces deformations and increases computational costs and time. To achieve a successful model it is essential to vary the mesh size in certain areas, this mesh refinement should take place in regions such as compression zones and other areas of complex behaviour.

In NLFEA, the loads are increased step by step until the structure experience a structural failure. There are many types of iterative to solve the equations in the analysis such as Newton-Raphson algorithm, modified Newton-Raphson algorithm and Riks Arc Length method. The finite element method changed drastically the way non-linear behaviour due to our understanding of the effect changes in geometry (stability considerations), due to deformation and displacements caused by loads, and due to the non-linear material properties. Instead of being able to predict only the

ultimate load and failure mechanism for structural members or to estimate buckling loads under a number of simplifying assumptions, one can follow the behaviour of complex structures as the loads increase and it undergoes inelastic deformations, until a limiting condition is reached.

2.6.2 Finite Element Modelling

The analysis begins by making a finite element model of the device. The model is an assemblage of finite elements, which are pieces of various sizes and shapes. The finite element model contains the following information about the structures to be analysed:

- I. Geometry to be subdivided into finite elements
- II. Material to included depending an mode of analysis of linear or non-linear
- III. Excitations to be excite as displacement on loading
- IV. Constraints to hold the structures depending on degree of freedom chosen.

Material properties, excitation, and constraints can often be expressed quickly and easily, but geometry is usually difficult to describe depending on the complexity of the model.

2.6.3 Computer Program for the Finite Element Analysis

There are numerous vendors supporting finite element programs, and the interested user should carefully consult the vendor before purchasing any software. However, to give an idea about the various commercial personal computer programs now available for solving problems by the finite element method. The existing programs that be used for solving finite element problem are, ALGOR, ANSYS, COSMOS/M, STARDYNE, IMAGES-3D, MSC/NASTRAN, SAP90 and GT-STRU DL.

Standard capabilities of many of the listed programs include information on: -

- Element types available, such as beam, plane stress, and three-dimensional solid.
- Type of analysis available, such as static and dynamic.
- Material behaviour, such as linear-elastic and nonlinear.
- Load types, such as concentrated, distributed, thermal, and displacement (settlement).
- Data generation, such as automatic generation of nodes, elements, and restraints (most programs have preprocessors to generate the mesh for the model).
- Plotting, such as original and deformed geometry and stress and temperature contours (most programs have postprocessors to aid in interpreting results in graphical form).
- Displacement behaviour, such as small and large displacement and buckling.
- Selective output, such as at selected nodes, elements, and maximum or minimum values.

All programs include at least the bar, beam, plane stress, plate-bending, and three-dimensional solid elements, and most now include heat-transfer analysis capabilities.

CHAPTER 3

MODELLING OF THE DIAPHRAGMS AND THREE DIMENSIONAL FRAME

3.1 Introduction

Most finite element software package like ABAQUS, ALGOR, ANSYS, COSMOS/M, STARDYNE, ADINA, MSC/NASTRAN, SAP90 and GT-STRUDL are able to carry out a nonlinear finite element analysis. These programs provide different types of elements for one-, two- or three dimensional problems such as plane stress, plane strain, three dimensional solid elements, straight and curve beams, and shell elements. In this project, COSMOS/M (Version 2.0) has been selected for the purpose of analysing the effects of floor diaphragms to the lateral stability of multi-storey frames. This may due to its flexibility in geometric and analysis modelling.

In order to give a clear view of the working process, the modelling procedures including all parameters in the analysis will be described step by step in this chapter.

3.2 COSMOS/S Software

COSMOS/M is a complete, modular, self-contained finite element system which is developed by Structural Research and Analysis Corporation (S.R.A.C.) of California. The system is capable of solving linear, non-linear, static and dynamic problems, including fields of heat transfer, fluid mechanic and electromagnetic problems.

Full package of COSMOS/M contains of various modules, different modules for solving different problems. NSTAR is one of the modules available. The Nonlinear Structural Analysis Module (NSTAR) solves nonlinear structural static and dynamic problems. NSTAR would only work with the 64K version of GEOSTAR. However, there are limitation of nodes, elements, and volumes even in the full version of COSMOS/M, which is shown in the Table 3.1. Basically, there are three solution control techniques that can be applied in the analysis; force, displacement and arc length control.

Table 3.1: Limitation of entities in COSMOS/M

Entity	Limitation
Node	64 000
Element	64 000
Key Point	24 000
Curve	24 000
Surface	8 000
Volume	2 000

3.3 COSMOS/M Method

There are the numerous steps to use COSMOS/M for nonlinear analysis. Figure 3.1 shows the process of nonlinear analysis step by step.

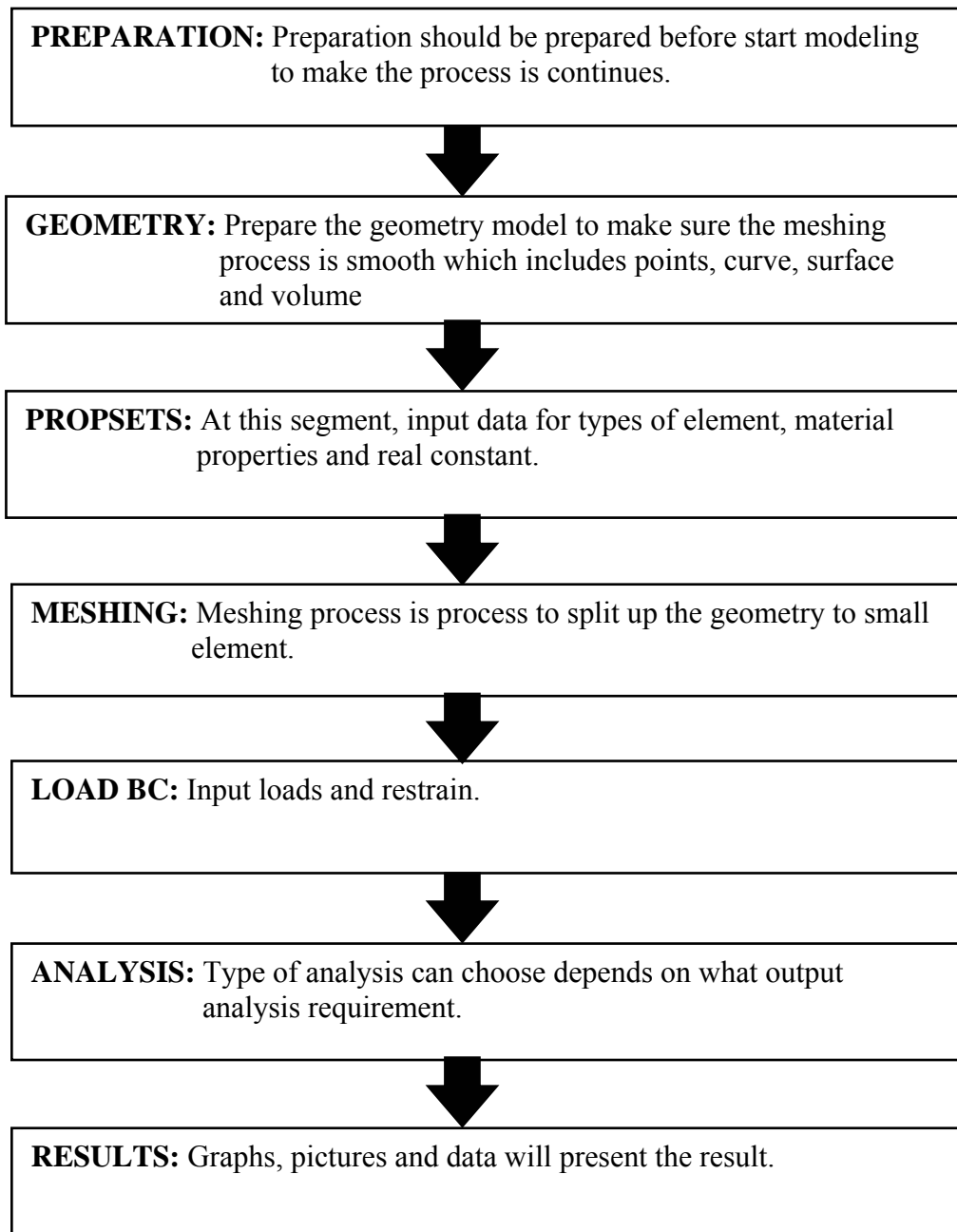


Figure 3.1: Analysis Steps using COSMOS/M

3.4 Finite Element Modelling

3.4.1 Element Shape

This section is the first step to model the structure and it is very important in the subsequent step for meshing. In COSMOS/M, the model is created starting with the definition of the points (PT), curves (CR), surfaces (SF) and volumes (VL). The COSMOS/M menu related to PT, CR, SF and VL is shown in Figure 3.2. The frame structure is modelled as a non-linear three dimensional (3D) model. Thus, the concrete element in finite element modelling can be modelled as a 20 Node 3D Solid Element (SOLID) which shows in Figure 3.3. Each node has three translational degrees of freedom whereby the three rotational degrees of freedom are constrained at each node. SOLID element is normally used in the analysis of structural, thermal and fluid models.

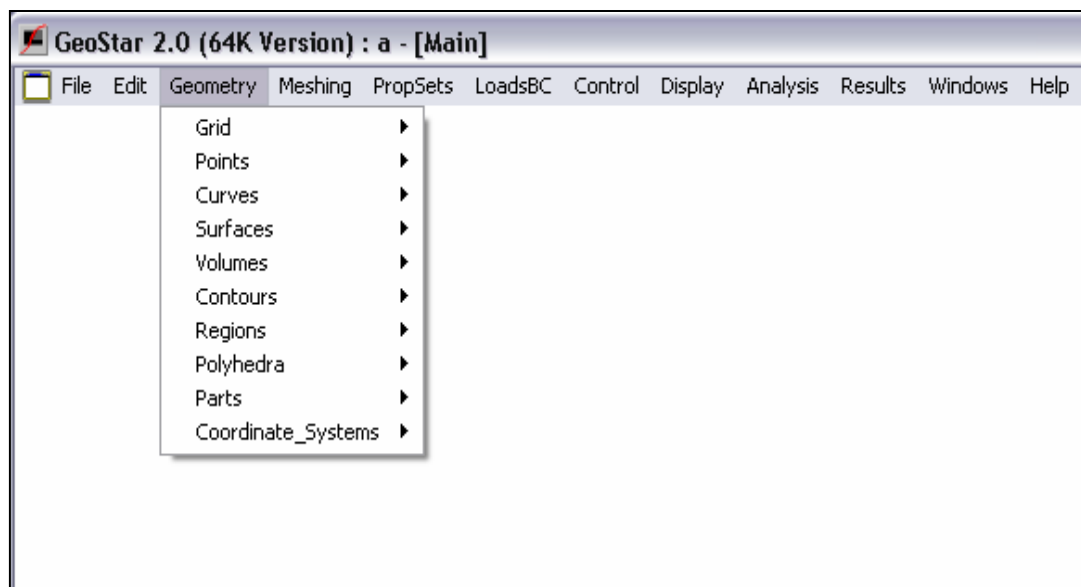


Figure 3.2: COSMOS/M menu related to PT, CR, SF and VL

The major difference between the capacity of a 3D solid element model and that of a 2D shell or plate element model lies on the stress states of the material under consideration. Unlike the 3D stress states in a solid element, the normal stress along the thickness direction in a shell element is basically neglected. As a result, the shell elements are not capable of accounting for the stress wave propagation in the target thickness direction. The solid elements have to be employed especially when the influence of normal stresses on the target failure cannot be ignored. Therefore in this study, the solid 3D elements have been adopted for model.

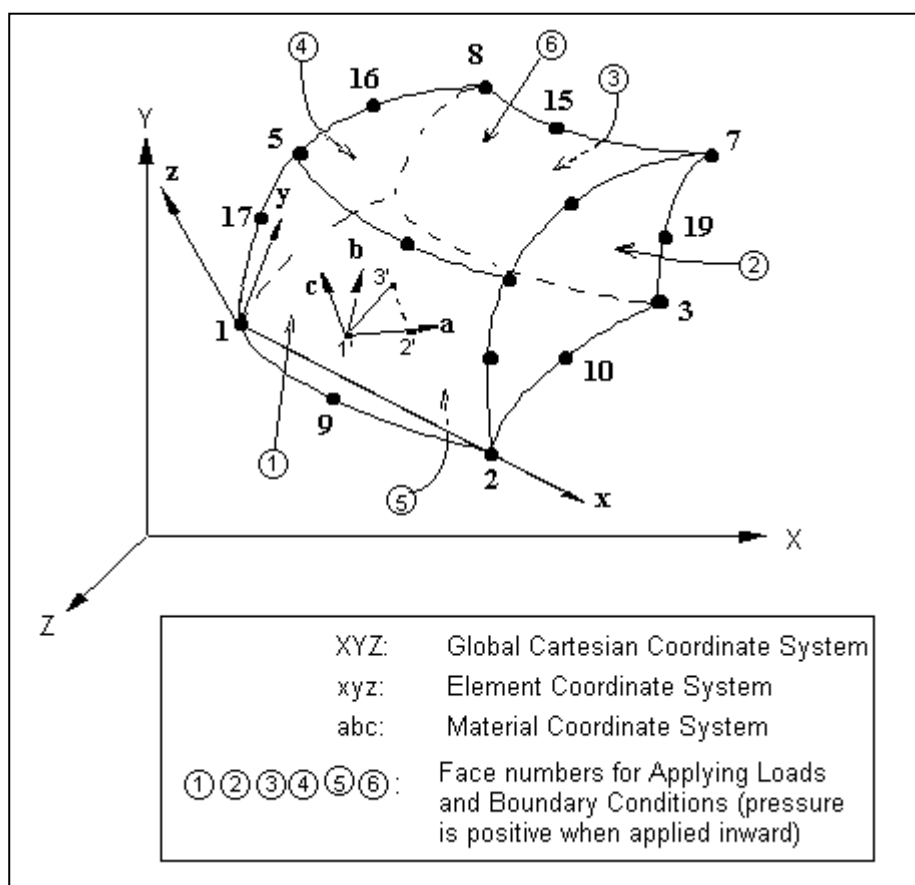


Figure 3.3: Description of the 3D Isoparametric Solid Element

3.4.2 Frame Geometry

The full scale finite element model of the structure model is as illustrated in Figure 3.4. The full model consists of 10 stories building height. The model is a 2 by 3 bay frame and the height between floors is 3135 mm. Table 3.2 shows the number of entities used in the frame structure model.

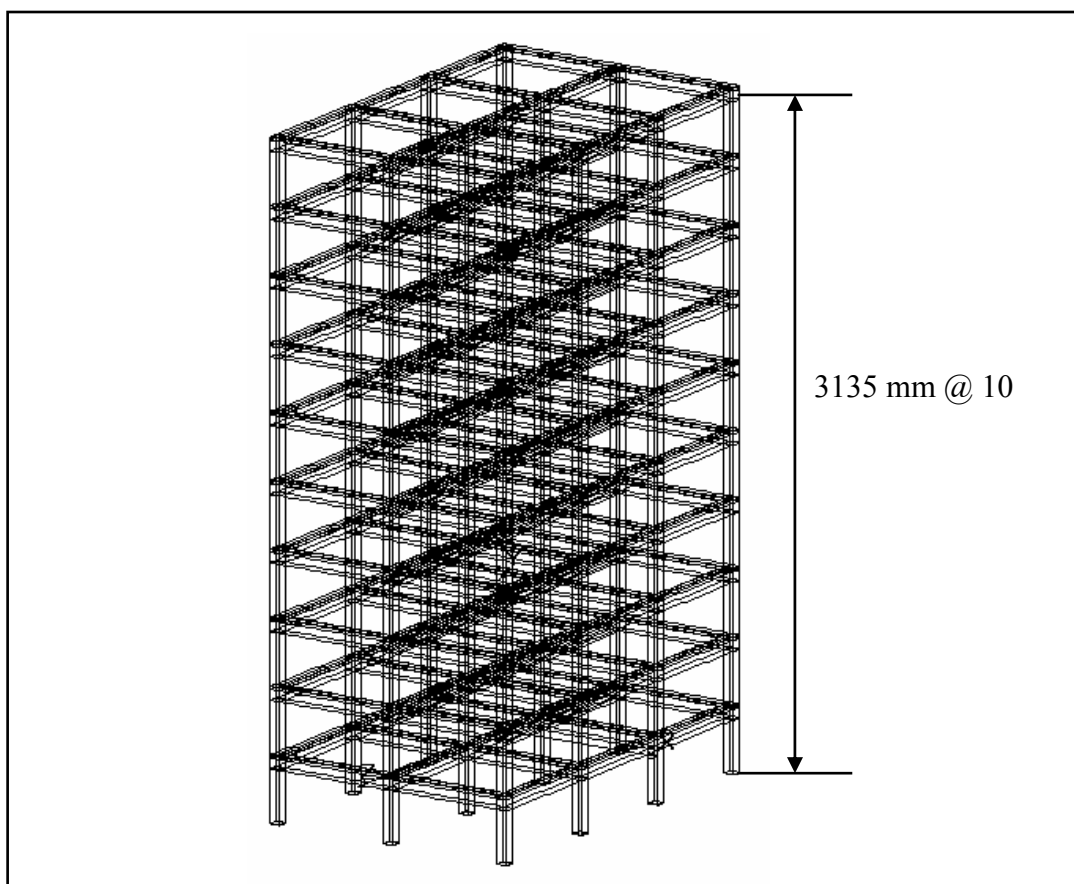


Figure 3.4: Frame structure geometry model by COSMOS/M

A typical floor layout of the 10 storey frame structure as illustrated in Figure 3.5 was used to investigate the influence of the flexural stiffness of slabs. The frame structure is modelled with the length of 18m and the width of 12m. The overall thickness of the slab is 135mm. The detail dimension of the frame structure is shown in Figure 3.6. All the beam in the frame structure comes with a same size which are 300 x 500 mm and the size of columns are 500 x 500 mm.

Table 3.2: Geometrical entities for the model

<u>Entity</u>	<u>Total number</u>
Point	1488
Curve	3956
Surface	3362
volume	760

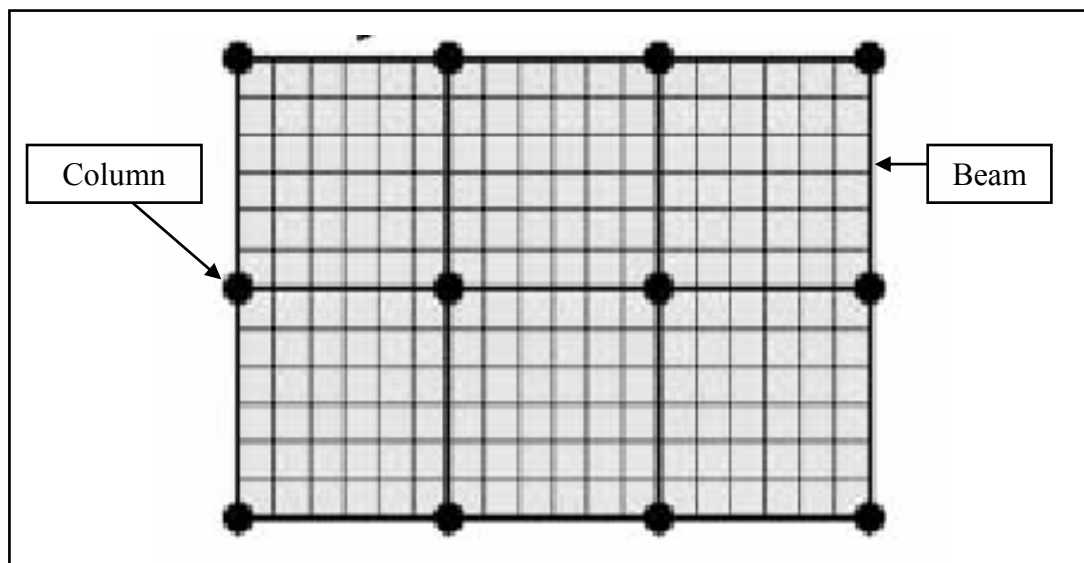


Figure 3.5: Plan view of the structures with a rigid slab diaphragm

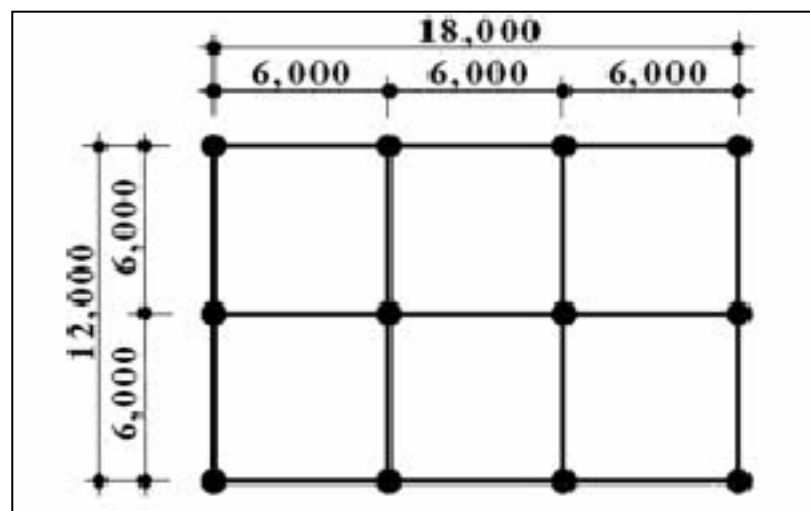


Figure 3.6: Plan Dimension

3.4.3 Material Properties

The proposed frame structure is a reinforced concrete structure. In this project, the main purpose is to investigate the effects of floor diaphragms to the lateral stability of multi-storey frames. Instead of providing two kind of materials; steel and concrete, a simplified method which is replacing the steel material by an equivalent concrete material can be applied. This can be done by modified the value of modulus of elasticity.

$$E_q = (1 - p)E_c + pE_s ;$$

p	=	% reinforcement
E _c	=	Modulus elastic for concrete
E _s	=	Modulus elastic for steel
E _q	=	Equivalent modulus elastic

Therefore, there is only one material; that is concrete, which is used in the frame model. Nonlinear elastic is assumed for this material. The material properties for concrete are listed as follows:

Properties of Concrete (Element Group 1)

Characteristic strength	:	35 N/mm ²
Modulus of elasticity	:	2.17 x 10 ¹⁰ N/m ²
Mass density	:	2400 kg/m ³
Poisson's ratio	:	0.2
Yield stress	:	15.63 x 10 ⁶ N/m ²

In COSMOS/M, the command RCONST (real constant) is set to represent the type and size of the associated elements. Self weight of concrete frame structure will be generated by COSMOS/M itself.

3.4.4 Material Curve for Concrete

Generally, for the nonlinear finite element analysis, the stress-strain curve for concrete shown in Figure 3.7 is adopted into the analysis. The stress-strain curve for concrete in compression was previously adopted by Abdul Kadir Marsono (2000) in his research work. This stress-strain curve is developed with reference to BS8110: Part 2: 1985 as shown in Figure 3.8. The adopted compressive strain at maximum stress (taken as $0.8f_{cu} = 28 \text{ N/mm}^2$) is 0.0022 and the ultimate strain is 0.0035. Figure 3.9 shows the COSMOS/M menu which used to include the stress-strain data in the analysis. The detail values of the stress-strain parameter can be referred to Appendix A.

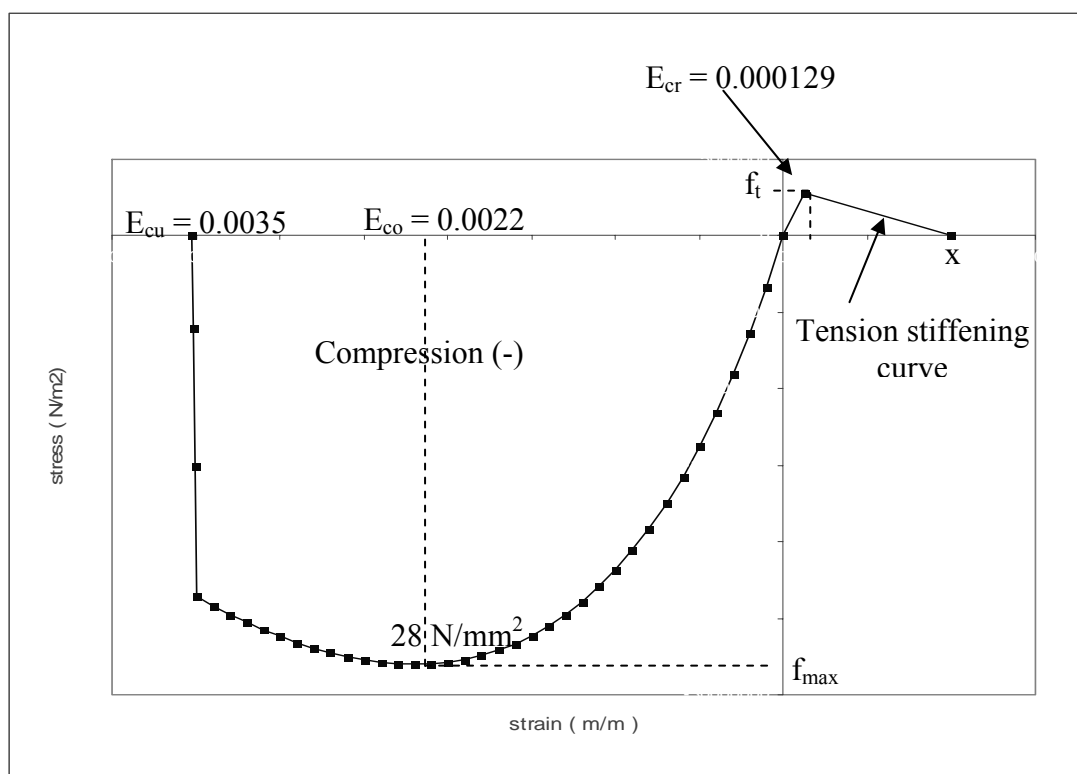


Figure 3.7: Stress-strain curve for concrete

In this case, concrete can be modelled using an anisotropic material model. Anisotropic model is generally used for materials that exhibit different yield and/or creep behaviour in different directions although concrete is generally treated as an

isotropic material. According to Shanmugam, Kumar, and Thevendran (2002), as the analysis progressed, cracking of concrete in tensile regions introduced instability in the numerical computations, which forced analysis to stop prematurely.

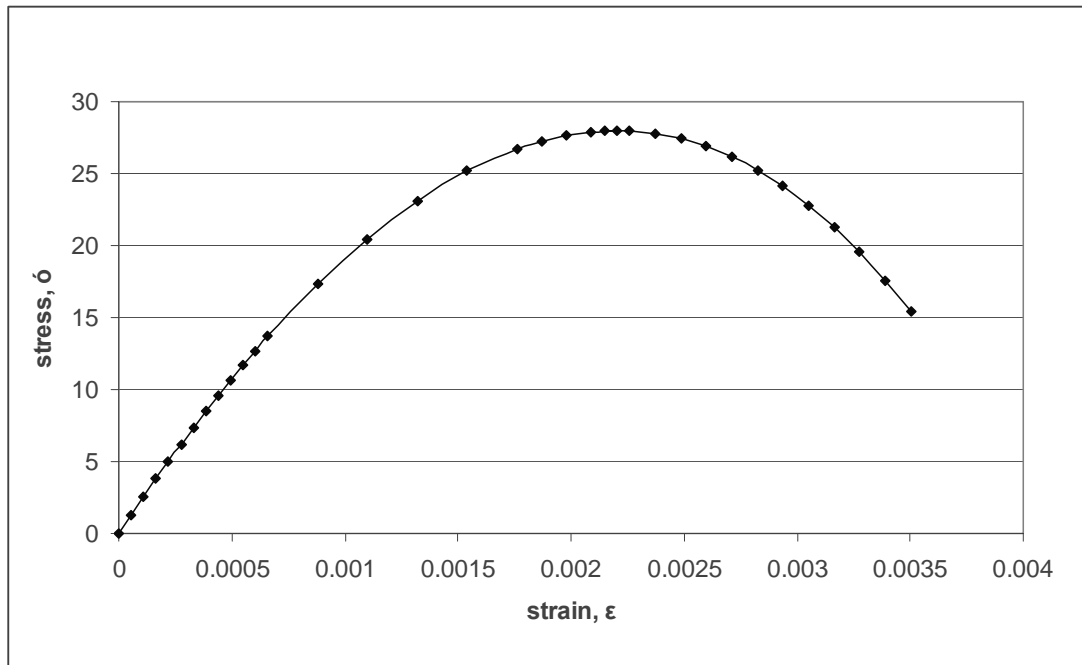


Figure 3.8: Stress-strain curve for concrete (Adopted from Marsono, 2000)

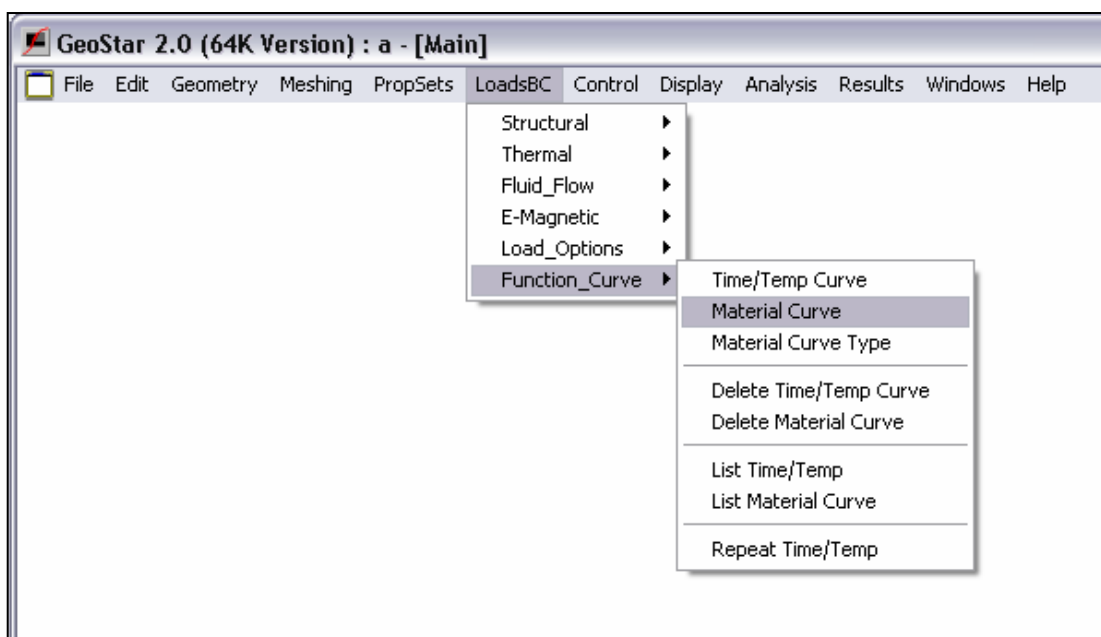


Figure 3.9: COSMOS/M menu related to the input of stress-strain data

“Tension stiffening” is a term used to describe the effect of interaction between reinforcing steel and concrete, once cracks have formed. When cracking occurs, concrete loses its continuity. As a consequence, the properties of concrete and the stress distributions in concrete and the reinforcing bars change greatly. In a concrete cracked zone, by the action of the bond stress at the interface between the reinforcing bar and concrete, the intact concrete between two adjacent cracks has the capacity to carry the tensile force transferred from the reinforcing bar. This capacity is called the tension stiffening effect (Chan, Cheung and Huang, 1993).

Analysis without considering the effect of tension stiffening is still valid. This is because neglecting the tension stiffening in the analysis is unlikely to effect the ultimate load predictions especially if the concrete element is ductile (Kotsovos and Pavlovic, 1995). However, in the real case, tension stress will continue to transfer between steel and concrete through its bonding action. Tension stiffening represents the degradation of concrete tensile strength between concrete and steel material which defines the post failure behaviour in tension after cracking has occurred.

According to Figure 3.7, the maximum tension stress for concrete, f_t , is assumed as 10% of the maximum compressive strength ($0.1f_{cu} = 3.5 \text{ N/mm}^2$). In reinforced concrete, the tension softening of the concrete is considering the effect of the tension stiffening. In order to determine the value for point x (strain value in tension at zero stress), the trial and converged method can be carried out.

3.4.5 Meshing

The process of meshing is to generate nodes and elements. A mesh is generated by defining nodes and connecting them to form elements. This means that, finer mesh will produce more accurate output.

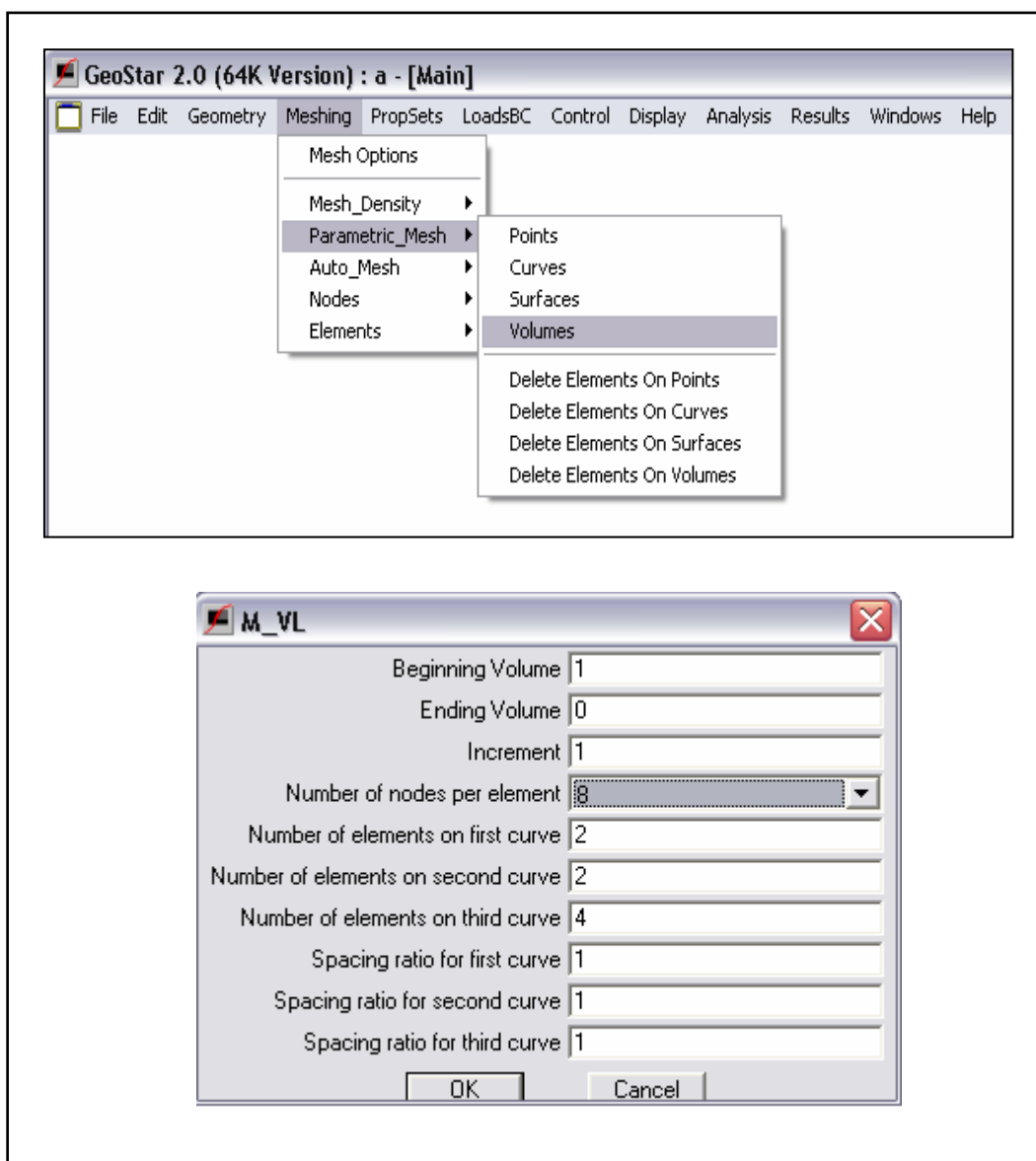


Figure 3.10: COSMOS/M menu for meshing

The element group, material properties and real constants are assigned to the geometry before generating the nodes and elements. By using the Parametric_Mesh command in COSMOS/M (Figure 3.10) with the mesh of 2-2-4 (x, y and z direction), the model is discretized into finite elements as shown in Figure 3.11 and Figure 3.12. The model was discretized into 12160 elements with 21498 nodes.

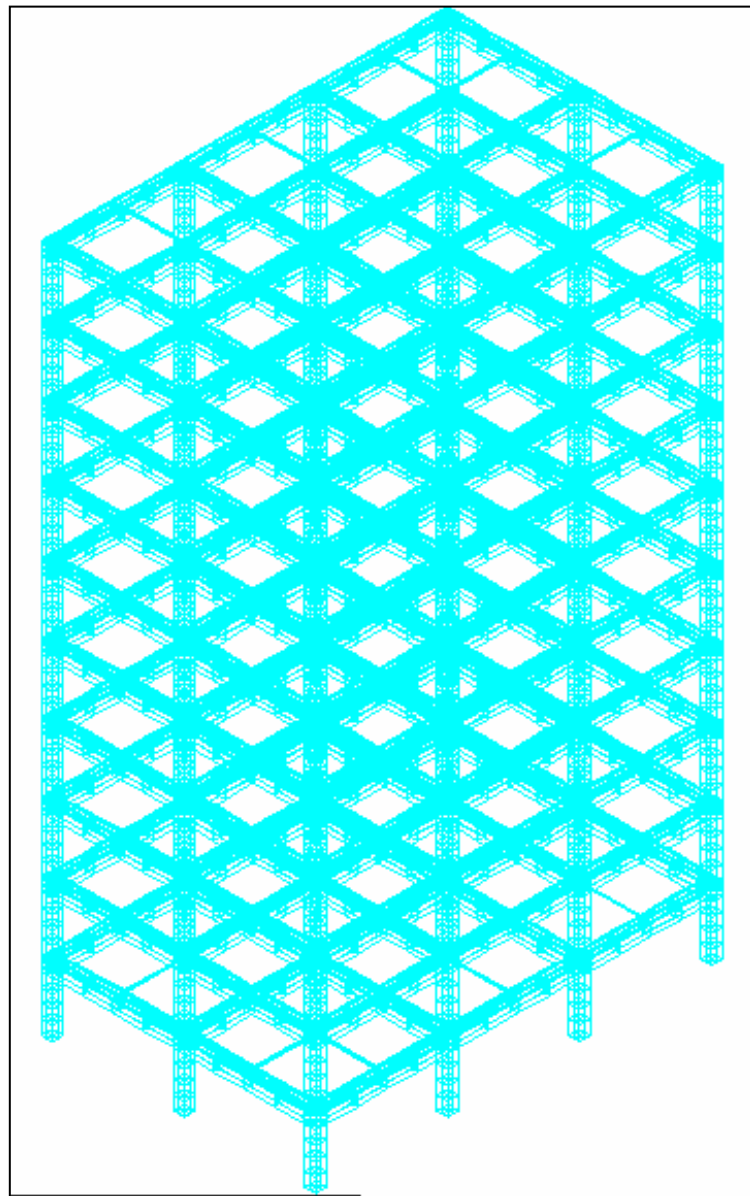


Figure 3.11: 3D view of the model after meshing

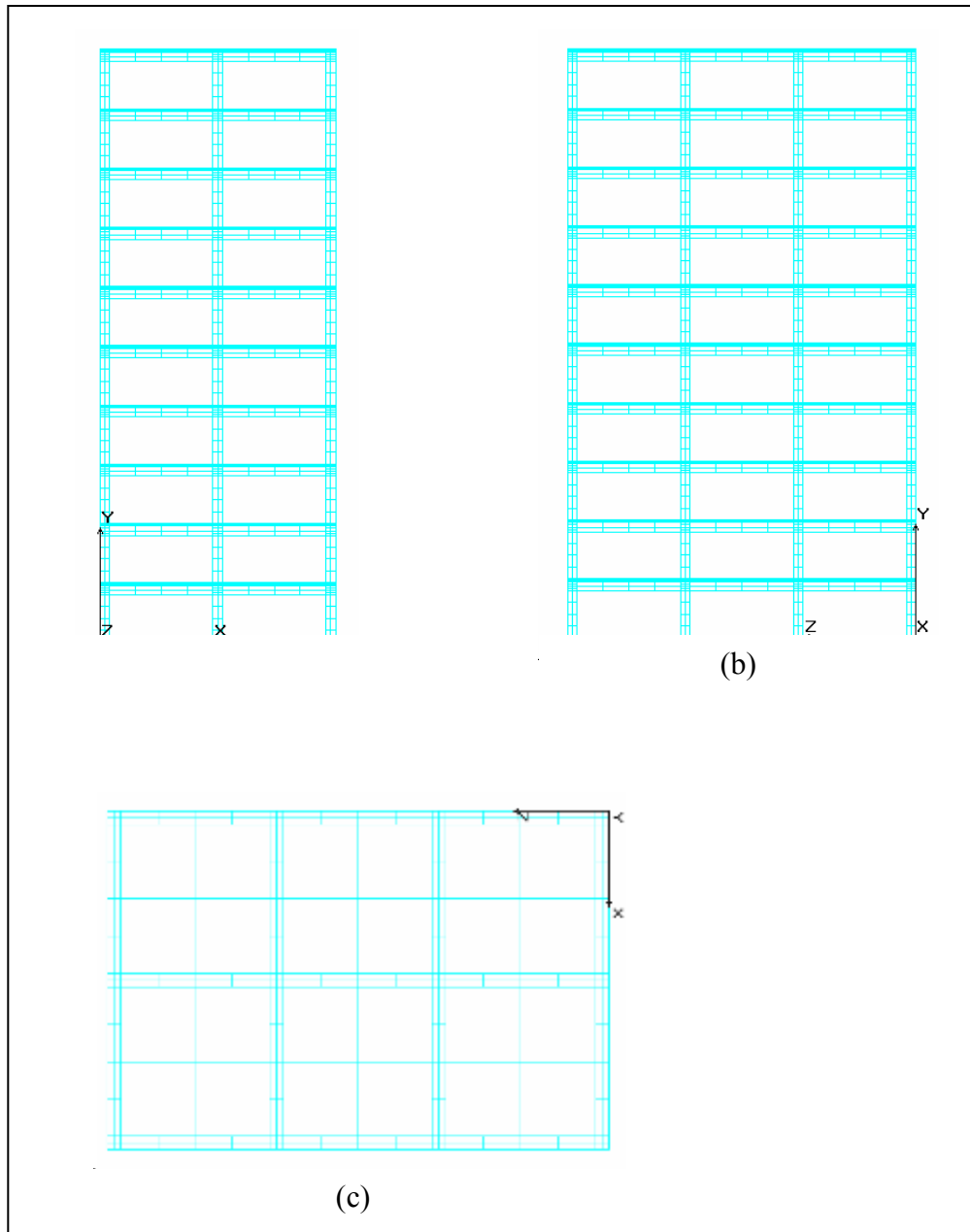


Figure 3.12: (a) Side view; (b) Front view and (c) Plan view

3.4.6 Boundary Condition and Loading

The software allows all input of restraints or loads at individual nodes and elements to be done directly to the selected entities. The directions of restraints and loading are interpreted with respect to the active coordinate system. Figure 3.13

shows the restraints of the model. Since the connections of the frame are assumed fixed with the foundations, therefore all the nodes are constrained in all degree of freedoms (that is all 6 DOF).

The main loading for the frame structure is lateral wind load. With regard to this, in Malaysia a typical distribution load of 922 N/m^2 is adopted for tall building analysis in accordance with CP3: Chapter V: Part 2: 1972. The total loading is applied to all nodes associated with the specified geometric entities.

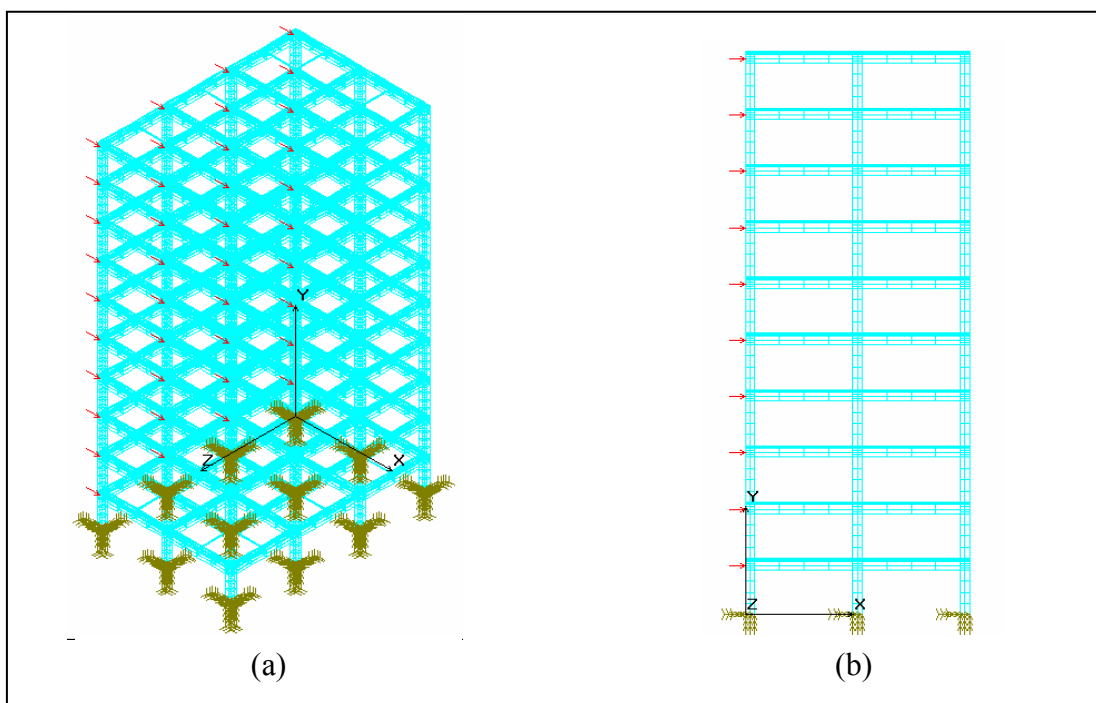


Figure 3.13: Loadings and restraints of model; (a) 3D view and (b) Side view

3.4.7 Solution Procedures

There are different numerical procedures that can incorporate in the solution of nonlinear problems using finite element method. A successful procedure must include the following:

- a) A control technique capable of controlling the progress of the computations along the equilibrium path(s) of the system.
- b) An iterative method to solve a set of simultaneous nonlinear equations governing the equilibrium state along the path(s)
- c) Termination criterias to end the solution process

Nonlinear solution technique and overall nonlinear solution strategy to be adopted are the most important for nonlinear pre- and post-yielding analyses of concrete members.

3.4.7.1 Arc Length Control

From the three solution control methods available in COSMOS/M (Figure 3.14), the arc length method is selected as the increment control technique for analysis used in this study. In the geometric sense, the control parameter is as a set of equations governing the equilibrium of the system which can be viewed as an ‘arc length’ of the equilibrium.

The Riks algorithm in COSMOS/M can be used to obtain static equilibrium in nonlinear unstable regions, thus facilitating the tracing of load deflection

behaviour up to collapse and beyond. This method is effective for large scale, mildly nonlinear problem and can handle the strain softening behaviour of concrete. Arc length method could also overcome the problem of non-positive definite stiffness matrix. Thus, there will not be a case of iteration and solution process stop when the stiffness matrix becomes negative or zero in the unstable region of the stress-strain curve. This advantage is achieved because both the load and displacement parameters are kept as variable in arc length method.

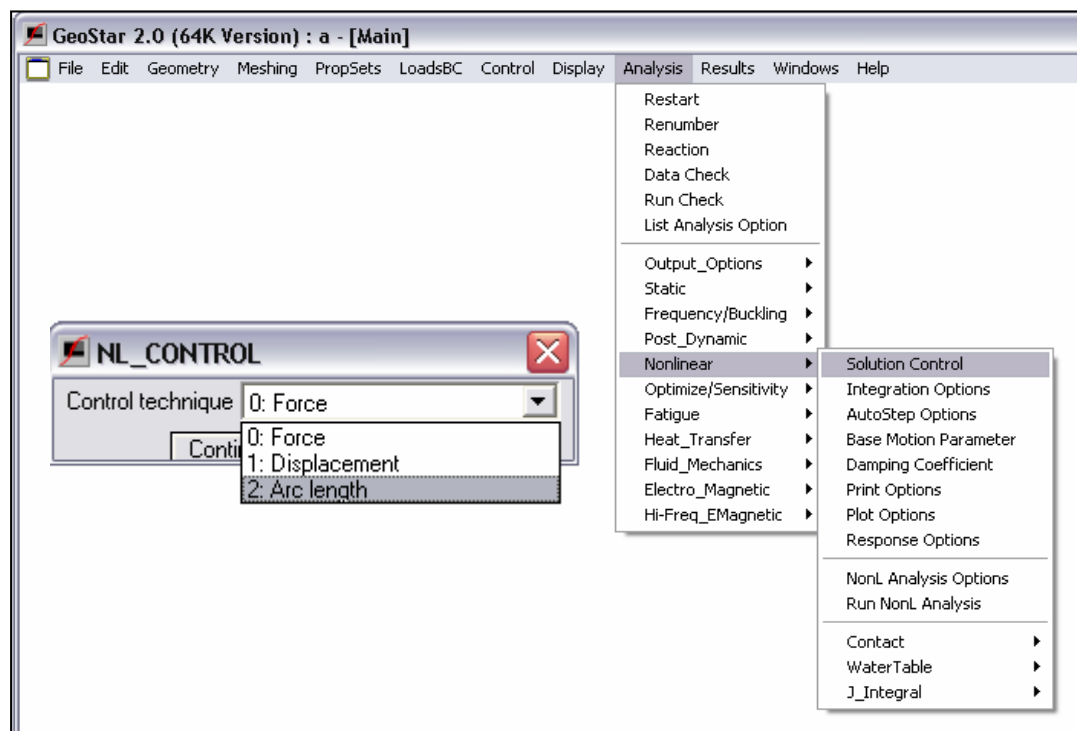


Figure 3.14: COSMOS/M menu which shows the Arc-length method

3.4.7.2 Iterative Solution Method

Several numerical difficulties are observed in nonlinear solution process even if arc-length method is used. Load factor may become negative or regression in the solution process may occur. COSMOS/M employs the Newton-Raphson (NR) approach (Figure 3.15) to solve nonlinear problems. In this approach, the load is

subdivided into a series of load increments. The load increments can be applied over several load steps.

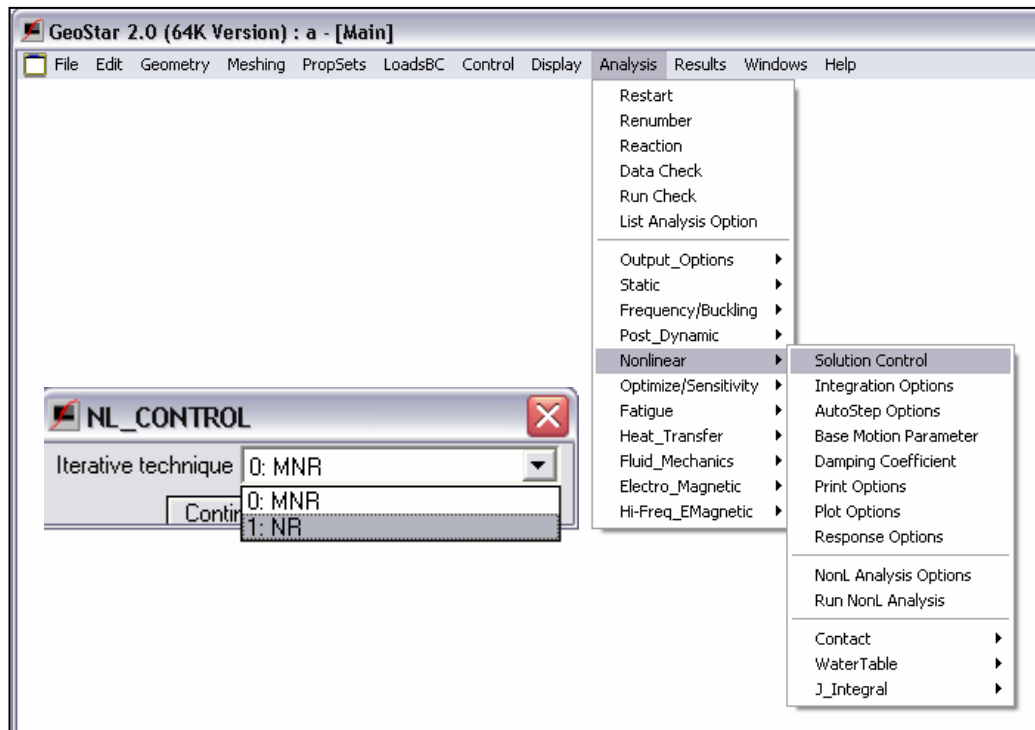


Figure 3.15: COSMOS/M menu which shows the NR method

Before each solution, the NR method evaluates the out-of-balance load vector, which is the difference between the restoring forces (the loads corresponding to the element stresses) and the applied loads. The function will then perform a linear solution, using the out-of-balance loads, and check for convergence. If convergence criteria are not satisfied, the evaluation process is then repeated, the stiffness matrix is updated, and a new solution is obtained. The iterative process continues until the convergence is satisfied. If the tangent stiffness (the slope of the force-deflection curve at any point) is zero, convergence will not be possible. This is shown as Figure 3.16.

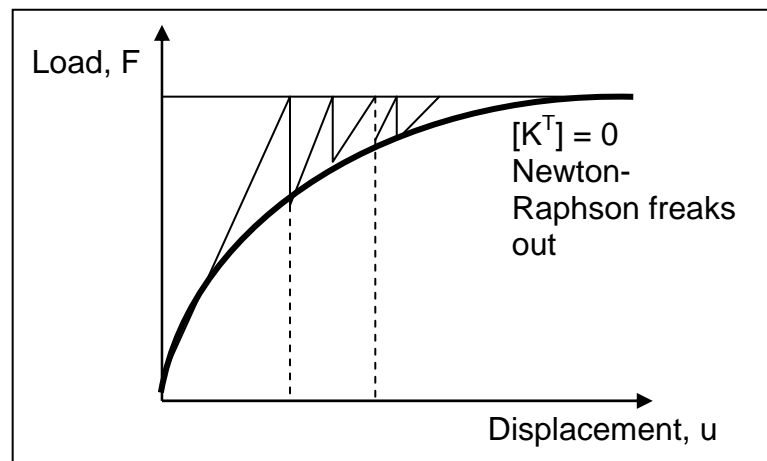


Figure 3.16: Modified Newton-Raphson Method

The tangent stiffness matrix may become singular or non-unique if the NR method is applied alone. This may occur in some certain case of analysis. Consequently convergence is hard to achieve. Therefore, arc-length control method is activated as an alternative iteration function to help avoid bifurcation points and track unloading. The arc length method causes the equilibrium iterations to converge along an arc, thereby often preventing divergence, even when the slope of the load vs. deflection curve becomes zero or negative. The NR method increases the load a finite amount at each sub-step and keeps that load fixed throughout the equilibrium iterations.

3.4.7.3 Termination Criteria

As stated earlier, a successful procedure must include the termination criteria or schemes. As the load increases during the iteration, each step of computation is checked whether convergence criteria are achieved. The analysis will be terminated if the system converged. Table 3.3 shows the termination criteria for the analysis in this study. This function must be activated using the command **NL_CONTROL** (Figure 3.17).

Table 3.3: Input data for nonlinear solution control

Parameter	Input in analysis
Maximum load parameter	1.0×10^8
Maximum displacement	50 (mm)
Maximum number of arc step	50
Average number of iterations per step	5

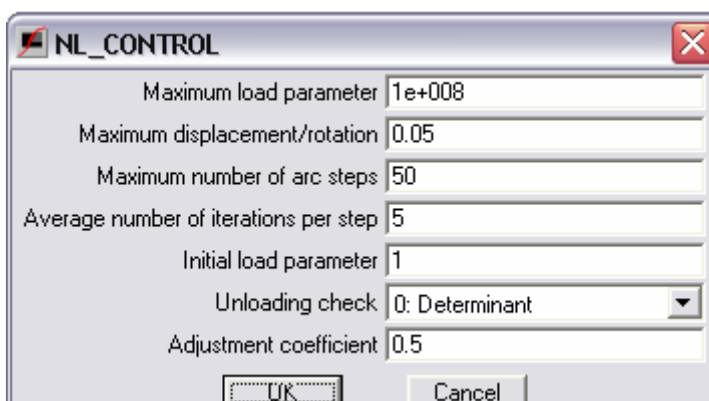


Figure 3.17: COSMOS/M menu for NL_CONTROL command

Analysis will be automatically terminated if any of the input exceeded during solution procedures. Besides the input stated in the table above, initial load parameter of 1.0 and convergence tolerance of 0.01 are also applied. The maximum deflection of 50 mm is calculated by dividing the building height with 1000. The deflection input is as initial guide for the nonlinear analysis to terminate. But the actual failure of the frame is depending on the stresses occur. The ‘automatic stepping technique’ or auto step function will automatically specify the load and/or displacement increment based on the specified parameters.

3.4.8 Results

All available results from the nonlinear analysis computed will be notified to the user when the command “Results > **Available Results**” is selected (Figure 3.18). The results in COSMOS/M can be obtained in various forms, such as graphical plot and listed in result windows. Model displacements and stresses may be listed or displayed using the commands provided in the “Results” submenu. Graphical plot results may be also performed to examine deformations, displacements, stresses and mode shapes of the slab model. For this study, results such as maximum and minimum principal stress for concrete are needed to determine the concrete failure in cracking and crushing respectively.

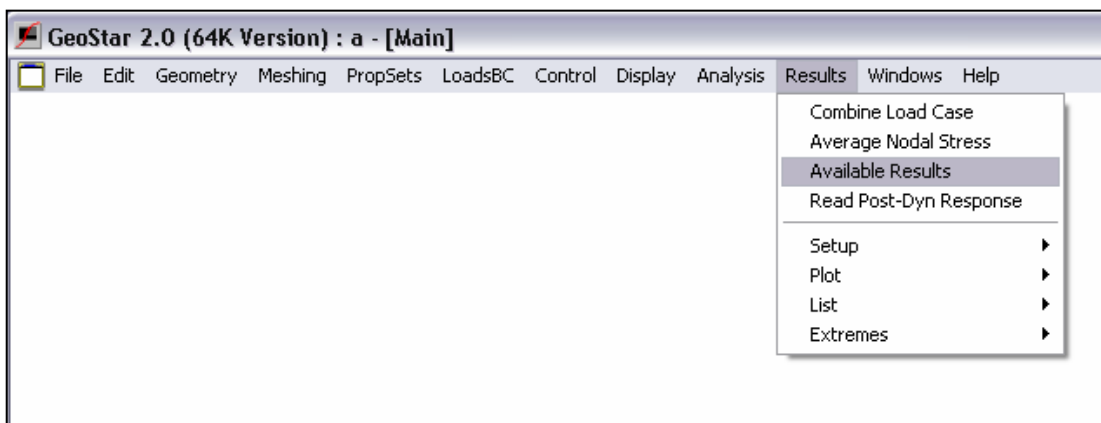


Figure 3.18: COSMOS/M menu for checking the available result

3.5 Conclusion

The results which are obtained from COSMOS/M are needed to be verified. For this study, the results from the nonlinear finite element analysis are compared with the results from Dong-Guen Lee (2002). The verification will be discussed in Chapter 4.

CHAPTER 4

VERIFICATION OF FINITE ELEMENT MODEL

4.1 Introduction

This chapter discusses the verification of the proposed finite element model in COSMOS/M. The verification can be carried out using available experimental or analytical results. In this study, the verification was done by comparing the results in COSMOS/M with the results from Dong-Guen Lee (2002). Once this is done, the results from COSMOS/M are adequate to use in the study of the effects of the floor diaphragms in multi-storey frames.

The process of verification is carried out by comparing the deformed shape of the floor diaphragms. The verification is based on the frame model with slabs.

4.2 Description of the Model

In this chapter, the frame model which will be discussed is shown as Figure 4.1. The full model consists of 10 stories building height. The model is a 2 by 3 bay frame and the height between floors is 3135 mm. The detail dimension and the material properties of the frame model have been mentioned in Chapter 3. The frame model was subjected to wind load of 922 N/m^2 .

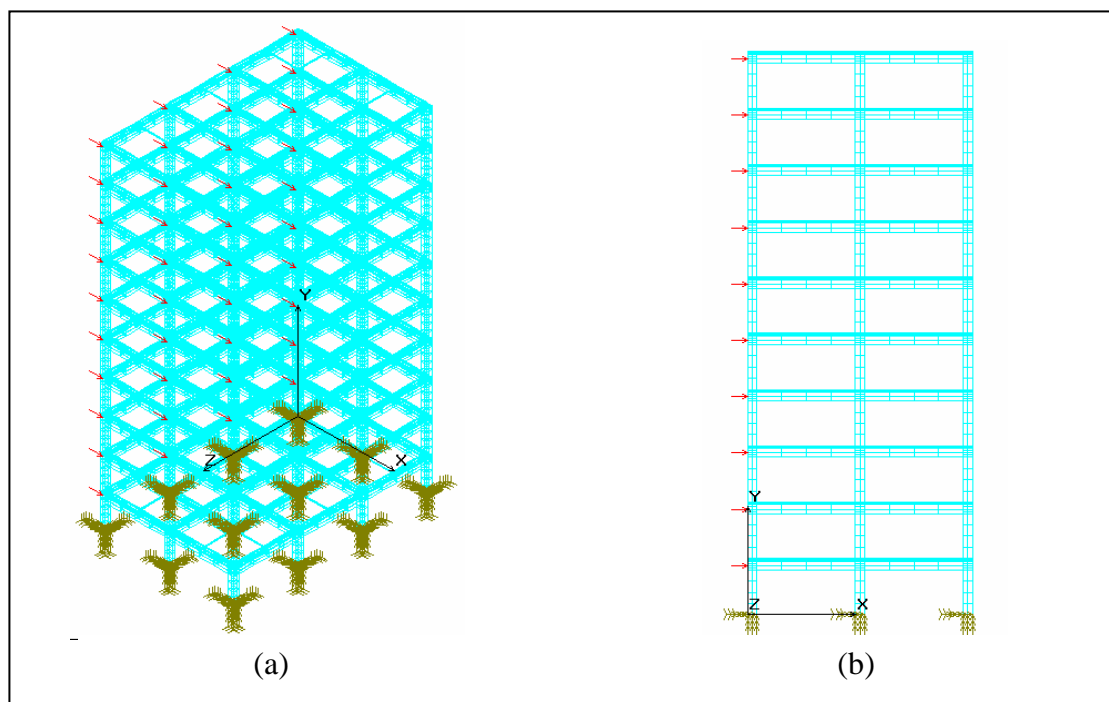


Figure 4.1: Loadings and restraints of model; (a) 3D view and (b) Side view

4.3 Comparison of Deformed Shapes of the Floor Diaphragms

In this study, the results from the nonlinear finite element analysis are compared with the results from Dong-Guen Lee (2002). Figure 4.2 shows the comparison of deformed shapes for the slabs. From the figure, it can be seen that the

deformed shape of the slabs obtained from the analysis is quite similar to the results from Dong-Guen-Lee (2002).

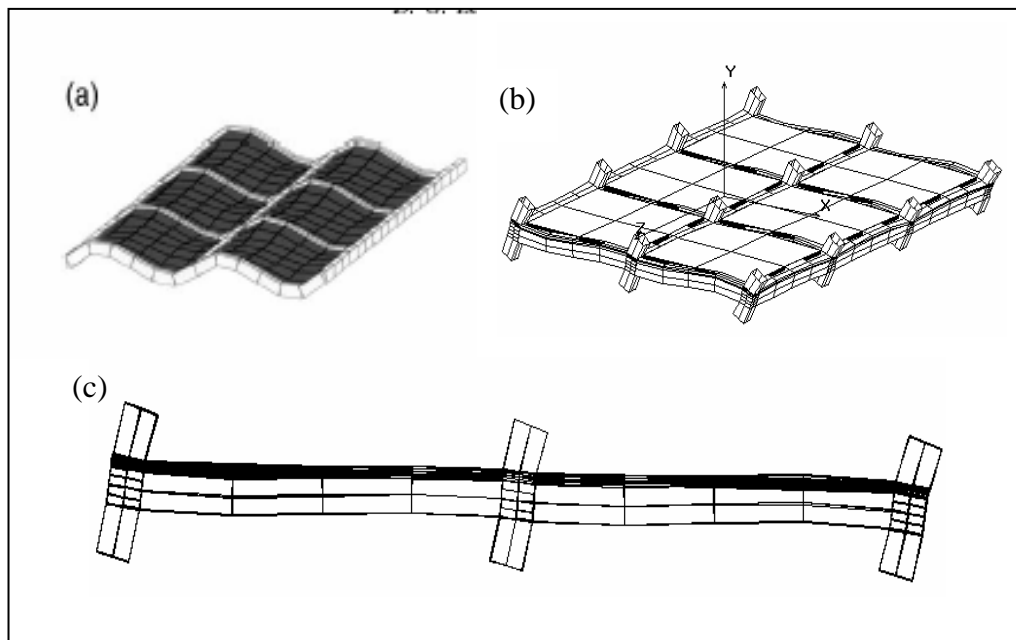


Figure 4.2: Comparison of the deformed shape for the slabs: (a) Result from Dong-Guen Lee, (b) Result from COSMOS/M (3D view), (c) Result from COSMOS/M (side view)

Furthermore, Figure 4.3 shows the comparison of deformed shapes of the global frame. It can be observed that the overall frame deformed shape obtained from the analysis is similar to the result of Dong-Guen Lee (2002).

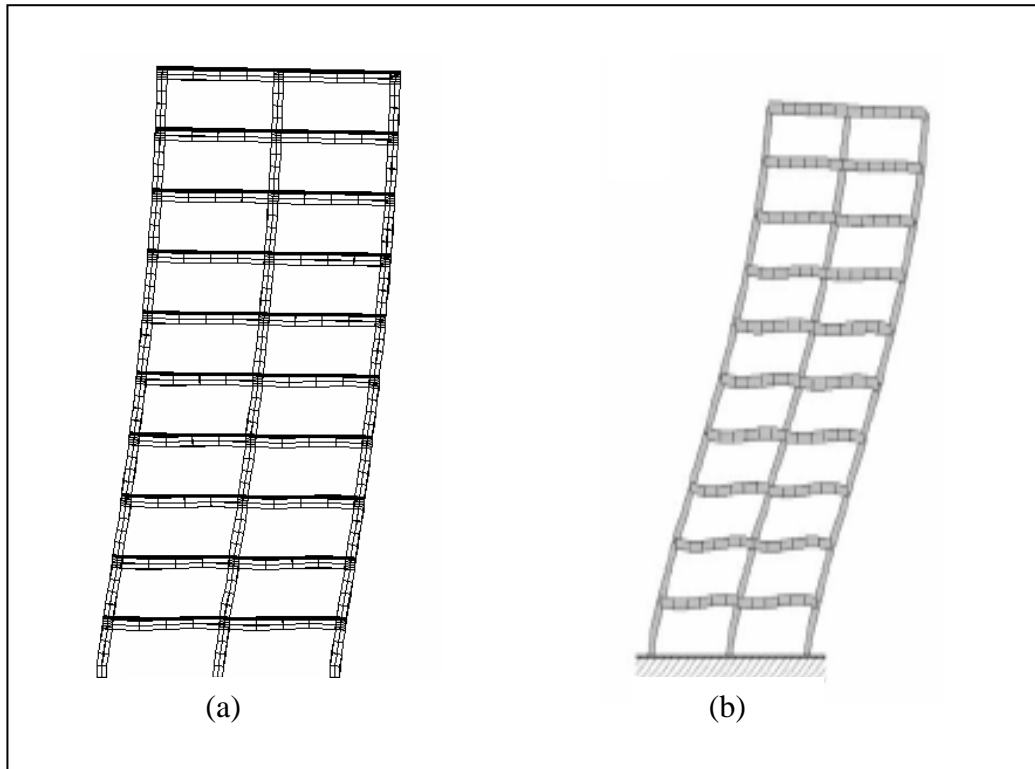


Figure 4.3: Comparison of the deformed shape for the global frame model:
 (a) Result from COSMOS/M; (b) Result from Dong-Guen Lee (2002)

4.4 Load-Deflection Characteristics of the Frame Structure

Figure 4.4 shows the comparison of load-deflection response between the analysis and Dong-Guen Lee (2002). From the figure, it is seen that the difference between the two maximum results is about 27%. These differences may be resulted due to several reasons as follows:-

1. The loads applied in Dong-Guen Lee's research are seismic load. Whereas, in this study, the seismic is replaced with an equivalent wind load.
2. There is a lack of information with regards to the frame model adopted by Dong-Guen Lee. Hence several assumptions have been employed in carrying out the actual model by the author.

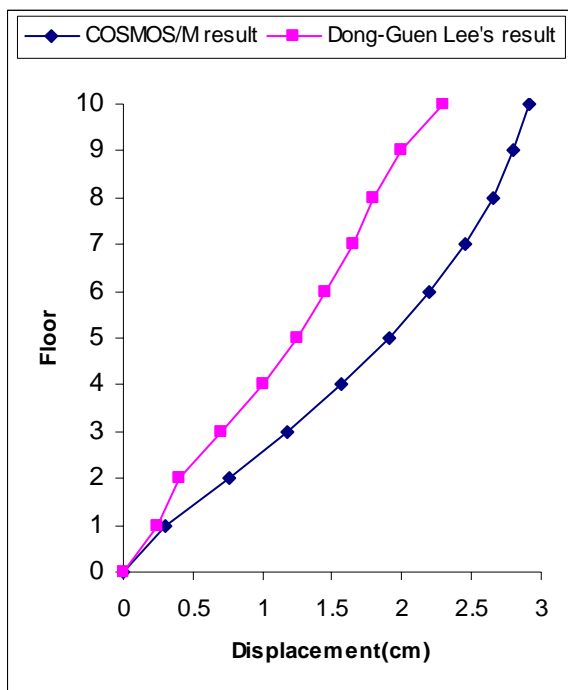


Figure 4.4: Comparison of displacement results between COSMOS/M and Dong-Guen Lee(2002)

However, the resultant forces have the same value with the applied forces in the analysis and the load-deflection characteristics of the frame structure have shown the nonlinear analysis is achieved.

4.5 Conclusion

In this study, the verification is done by comparing the proposed frame model with the results from Dong-Guen Lee (2002). It can be seen that the deformed shape of the proposed frame model is similar to Dong-Guen Lee's. In terms of frame deflection, the difference of the maximum deflection at story-10 is about 26% as compared to results obtained by Dong-Guen Lee (2002). Therefore the above verification shows that the modelling method, adopted by the author can be used to carry out further analysis as described in Chapter 5.

CHAPTER 5

LINEAR BEHAVIOUR OF FLOOR DIAPHRAGM

5.1 Introduction

Output from Linear Finite Element Analysis using COSMOS/M is discussed in this chapter. The wind load will be simplified to two point loads at the highest point of the frame (which is node 19732 and 19408). The results sought are resultant displacement, Von Mises Stress and In-plane Shear Stress. Displacement contour plots from COSMOS/M are employed to determine the maximum deflection of the frame structure. Thus, the effects of floor diaphragms in multi-story frame can be obtained by comparing the results between the frame structure with slab and without slab. Besides that, the stress contours from COSMOS/M shows the transmission of stress within the slabs, columns and beams. The floor diaphragm can be analysed by the strut and tie method or by considering the floor to act as a deep horizontal beam.

5.2 Load-Deflection Characteristics of the Frame Structure

Figure 5.1 shows the load-deflection response for the frame structure models under a constant loading of 500 kN. From the figure, the deflection of the frame with slabs is comparatively larger than the frame without slabs. Thus, this clearly shows that the slabs play important role in contributing the lateral stability to the frame structure. Table 5.1 shows the difference of the deflection between the two frame models.

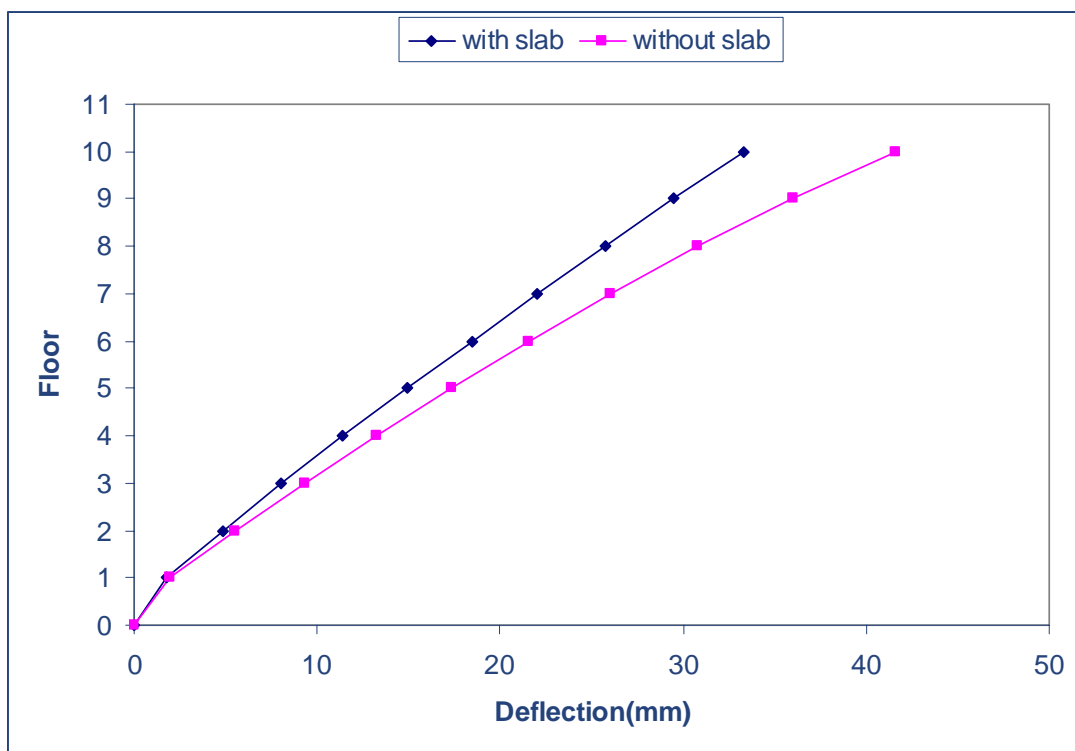


Figure 5.1: Deflection curve for frame structure under constant loading

Table 5.1: Comparison of frame deflections

<u>Floor</u>	<u>Displacement of frame with slab (mm)</u>	<u>Displacement of frame without slab (mm)</u>	<u>Difference (%)</u>
1	1.811	2.005	10.71%
2	4.829	5.523	14.37%
3	8.055	9.311	15.59%
4	11.41	13.25	16.13%
5	14.88	17.34	16.53%
6	18.43	21.58	17.09%
7	22.06	26.03	18.00%
8	25.74	30.79	19.62%
9	29.44	36	22.28%
10	33.26	41.61	25.11%

5.3 Output of Stress Analysis of the Frame Structure

5.3.1 Von Mises Stress

The main purpose for obtaining the static stress analysis result is to study the transfer of horizontal shear forces in the floor diaphragms. Figure 5.2 shows the contour plot of the Von Mises stress which can be important to describe the yield behaviour and consequently the failure criteria of the concrete. The figure shows that, all the stresses are concentrated at the column-beam connection and there is no stress in the middle of the slabs. The corresponding maximum Von Mises stress occurred at node 19732 and node 19408 with the value of 15.85 N/mm^2 for both nodes.

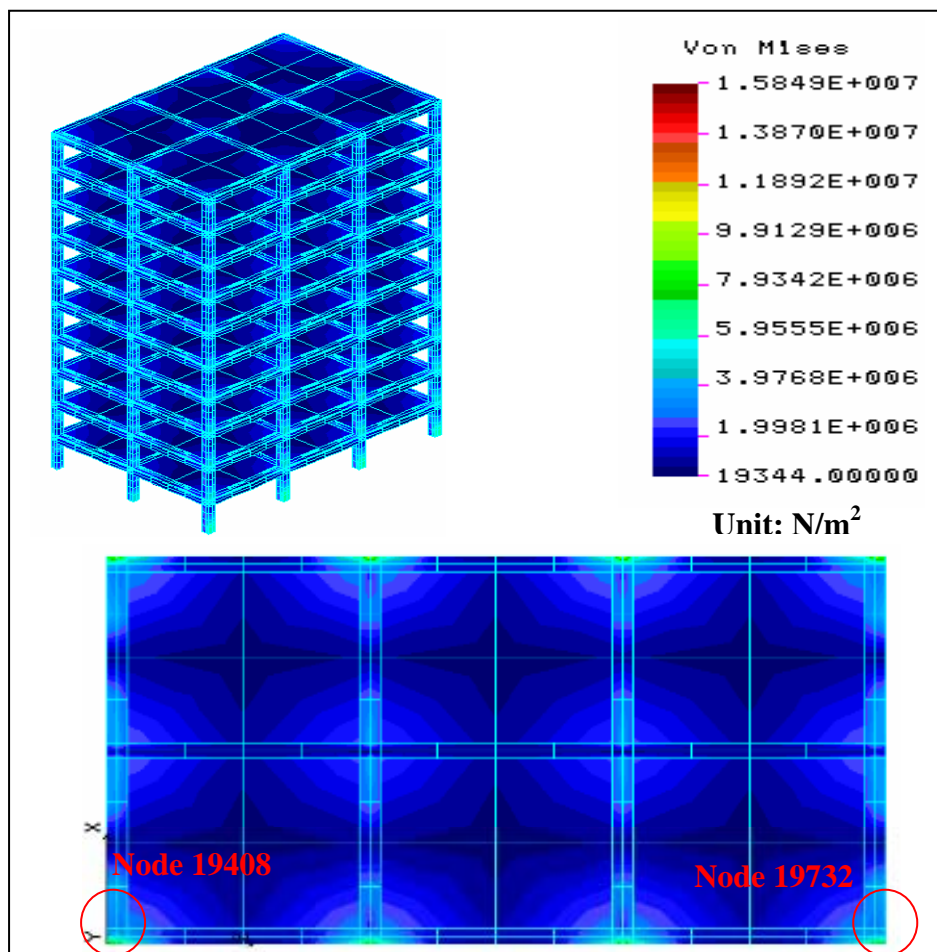


Figure 5.2: Contour plot of the von mises stress in 3D and plan view

5.3.2 In Plane Shear Stress

For the frame structure which includes the slabs, contour plot of the in plane shear stress under a scale factor of 10 is as shown in Figure 5.3. The maximum tension shear stress occurred at node 19405 (3.12 N/mm^2) and the maximum compression shear stress occurred at 19735 (-3.12 N/mm^2). In the frame structure, the slabs act as a deep beam to resist the horizontal forces. From the figure, it is clearly stated that the horizontal loads are transferred to the beams and columns by the slabs. This means that the horizontal forces will first transfer to the slabs then to the beams and columns.

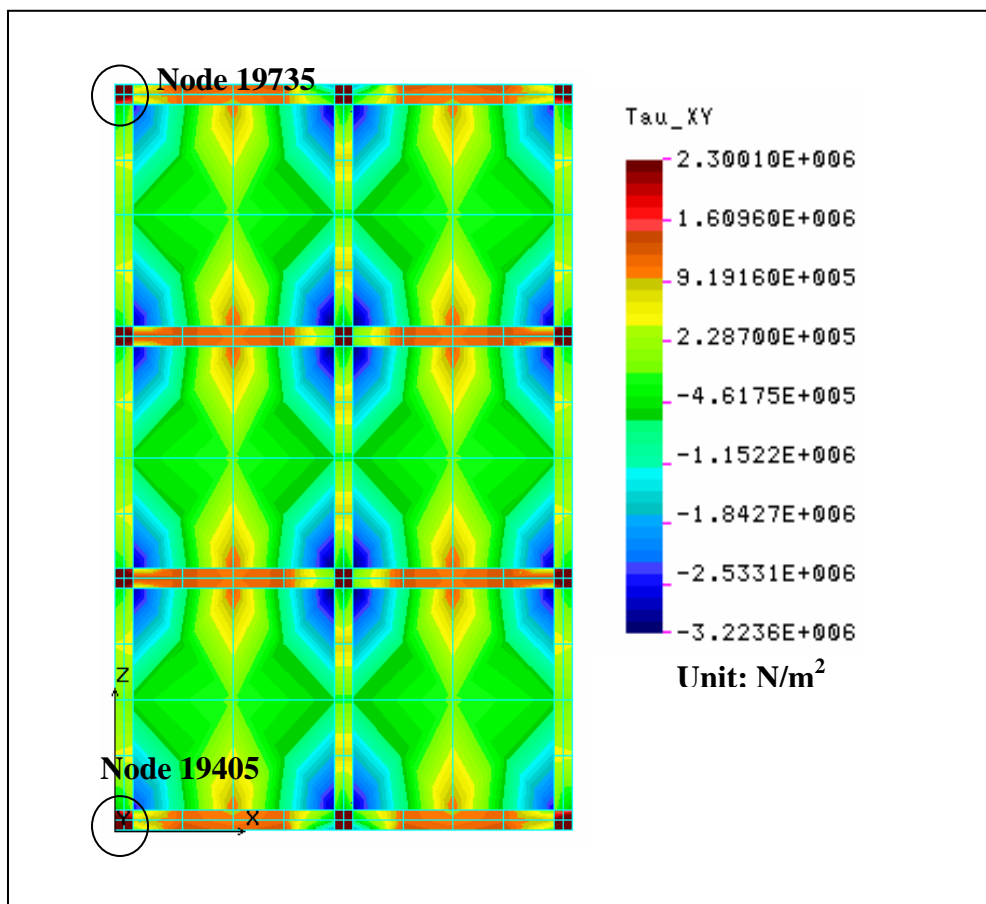


Figure 5.3: Contour plot of the in plane shear stress of frame structure with slabs

If the frame structure does not include the slabs, the horizontal loads will directly be transferred to the beams and columns. This response is shown in Figure 5.4. For the frame model without slabs, the maximum tension shear stress occurred at node 18703 (3.18 N/mm^2) and the maximum compression shear stress occurred at 19033 (-3.18 N/mm^2).

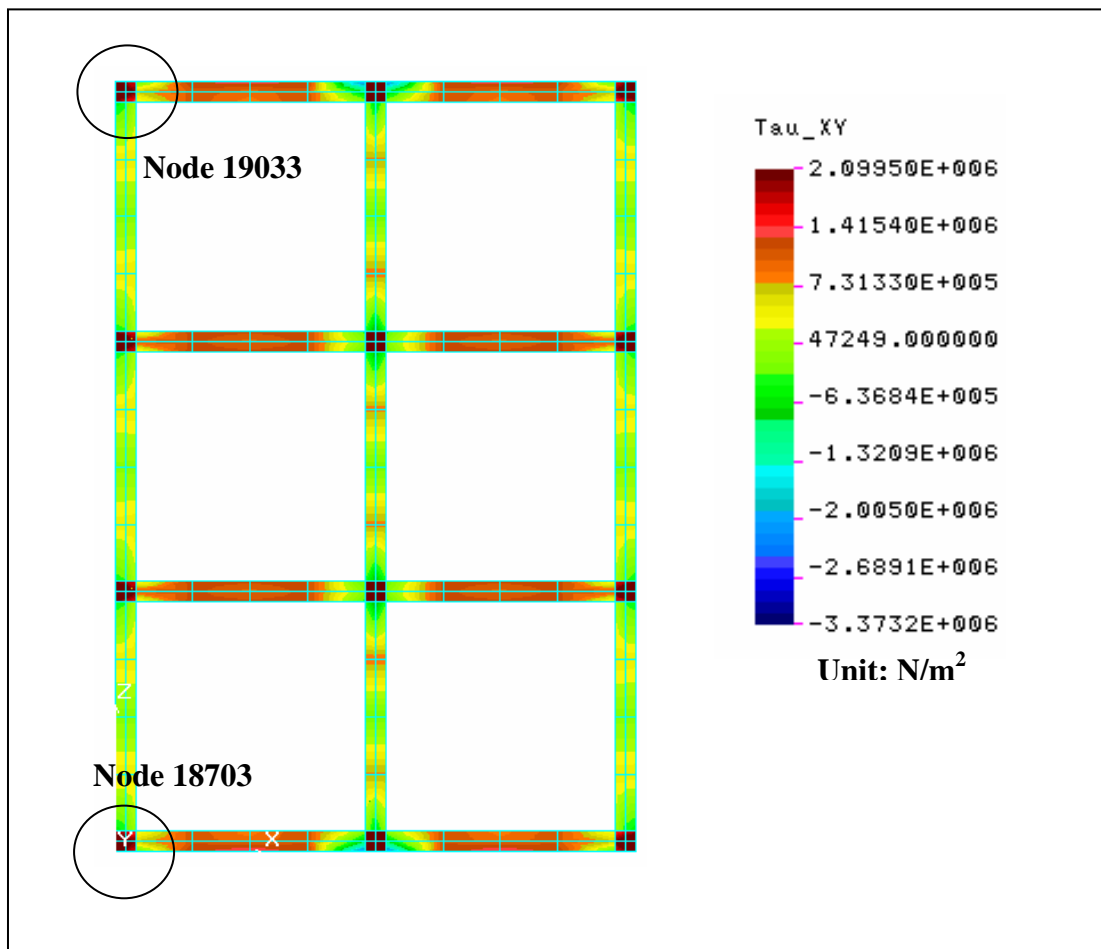


Figure 5.4: Contour plot of the in plane shear stress of frame structure without slabs

5.3.3 Diaphragm Action

Horizontal loads usually transmitted to the vertical cores or shear walls by the roof and floor acting as horizontal diaphragms. The floor can be analyzed by the strut and tie method or by considering the floor to act as a deep horizontal beam. The central core, shear walls or other stabilizing components act as supports with the lateral loads being transmitted to them as shown in Figure 5.5.

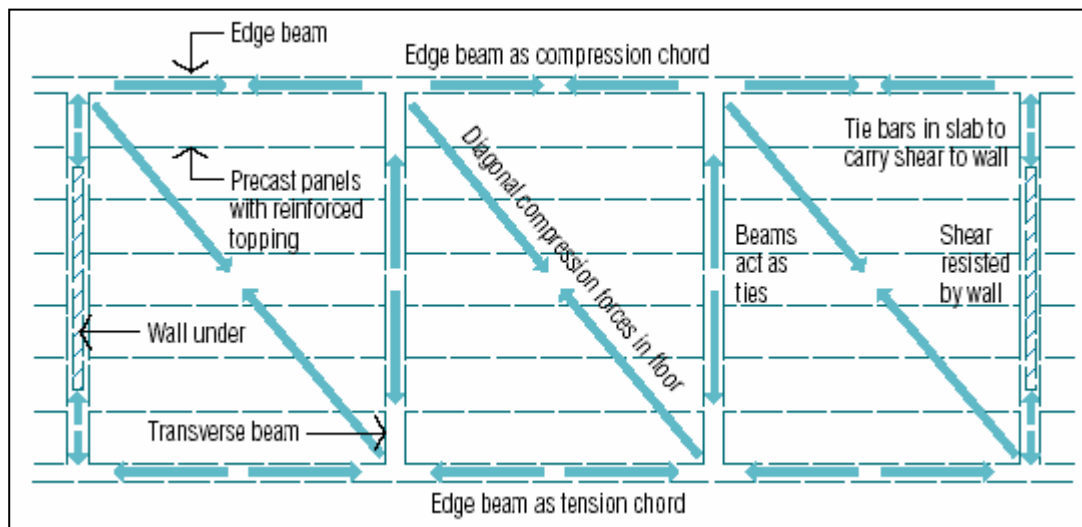


Figure 5.5: Actions in a diaphragm (Strut and Tie Model)

From the figure, it shows that the edge beam at the upper part is under compression stress and the edge beam at the lower part is under tension stress. Thus, it is clearly shows that the floor slabs is acting as a horizontal deep beam. Diagonal compression forces will occur at the slabs and the stresses in transverse beam is in tension. The slabs carrying the diagonal compression forces can be modelled as the strut. Whereas the transverse beams carrying the tension forces can be modelled as the tie.

By comparing Figure 5.5 and Figure 5.3, it shows that the transfer of the stresses in frame model is similar with the strut and tie theory. Therefore, the slabs in the frame model can act as a horizontal deep beam.

5.4 Conclusion

From the comparison of the two frame models, the slabs have increased the lateral stability performance of the frame structure by 10% to 25%. The slabs act as a horizontal beam to resist the lateral load. By using the strut and tie method, the slabs can be analyzed.

CHAPTER 6

NON-LINEAR BEHAVIOUR OF FLOOR DIAPHRAGMS

6.1 Introduction

Results from Nonlinear Finite Element Analysis using COSMOS/M are discussed in this chapter. The results sought are resultant displacement, maximum principal stress, P_1 , minimum principal stress, P_3 , and resultant stress (σ_x , σ_y , σ_z). Cracking failure of the frame structure will occur if the maximum principal stress, P_1 exceeds the value $0.1f_{cu}$. Crushing failure of the frame structure will occur if minimum principal stress, P_3 is less than $-0.8f_{cu}$. Maximum tensile stress and maximum compressive strength is recorded at the failure point. Displacement contour plots from COSMOS/M are employed to determine the maximum deflection of the frame structure. Thus, the effects of floor diaphragms in multi-story frame can be obtained by comparing the results between the frame structure with slab and without slab. Beside that, the stress contours from COSMOS/M shows the distribution of stress within the slabs, columns and beams.

6.2 Nonlinear Finite Element Analysis

6.2.1 Load-Deflection Characteristics of the Frame Structure

The load is increased automatically by the automatic stepping option using the **NL_AUTOSTEP** command. The minimum step increment input is $1.0e-8$ and the maximum step increment is equal to the maximum displacement defined in the arc length input **NL_CONTROL** command. The load-deflection response for the frame structure models are as presented in Figure 6.1. Figure 6.2 (a) and (b) shows the deformed shape of the frame structure.

Table 6.1: Comparison of frame deflections

<u>Load (kN)</u>	<u>Frame Deflection(mm)</u>		<u>Difference (%)</u>
	<u>With Slab</u>	<u>Without Slab</u>	
400	12.8	15	17.19%
800	25.9	30.2	16.60%
1200	39.1	46	17.65%

From Figure 6.1, the frame structure model which is including the slabs has higher ultimate load of 1437.35 kN and the ultimate load for the frame structure which is excluding the slabs is 1427.6 kN. For the deflection, it is clearly shown that the value for the frame structure model which is excluding the slabs is higher. Thus, it is proved that the lateral stability of frame structure has been increased by the slabs. Table 6.1 shows the difference of the deflection between the two frame structure models.

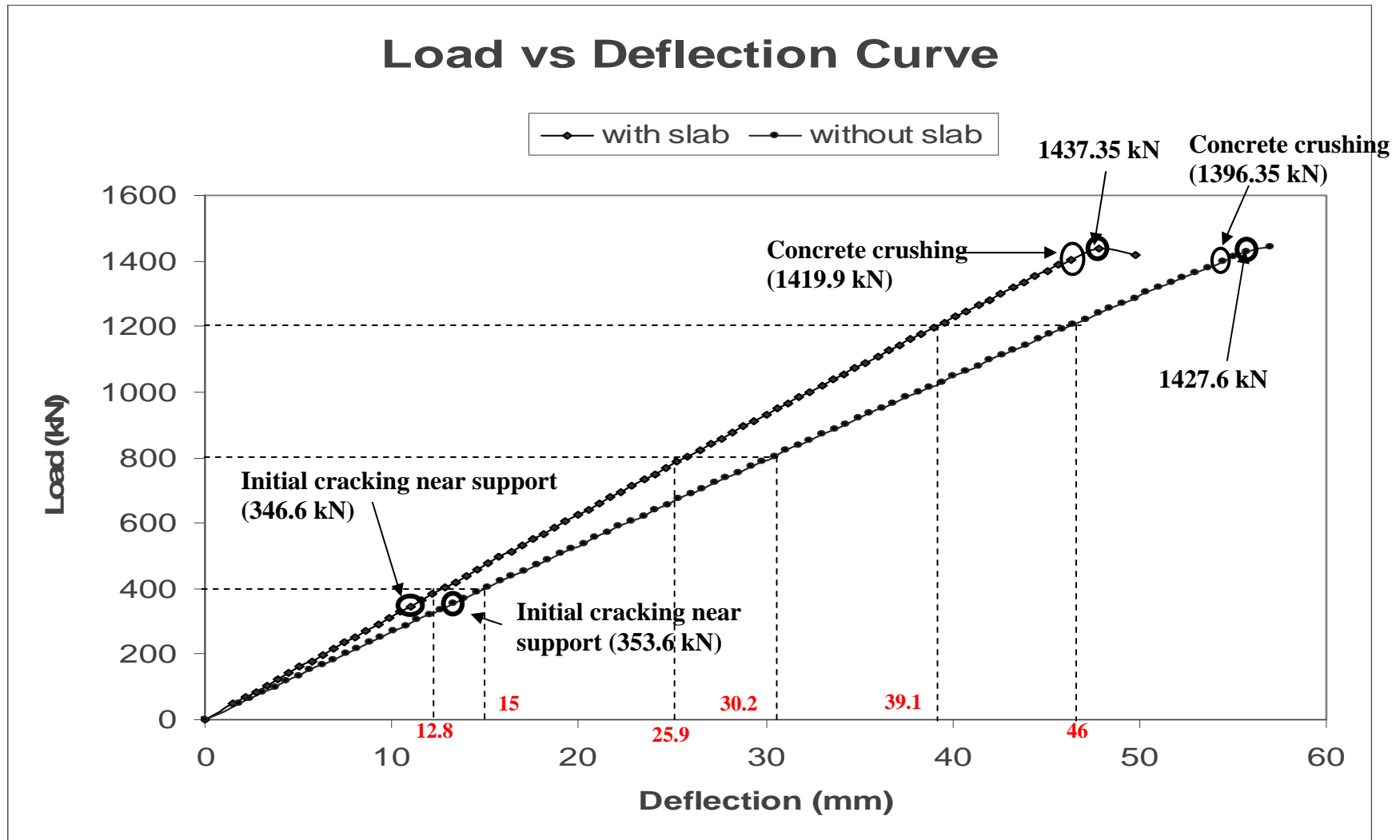


Figure 6.1: Load-deflection curve

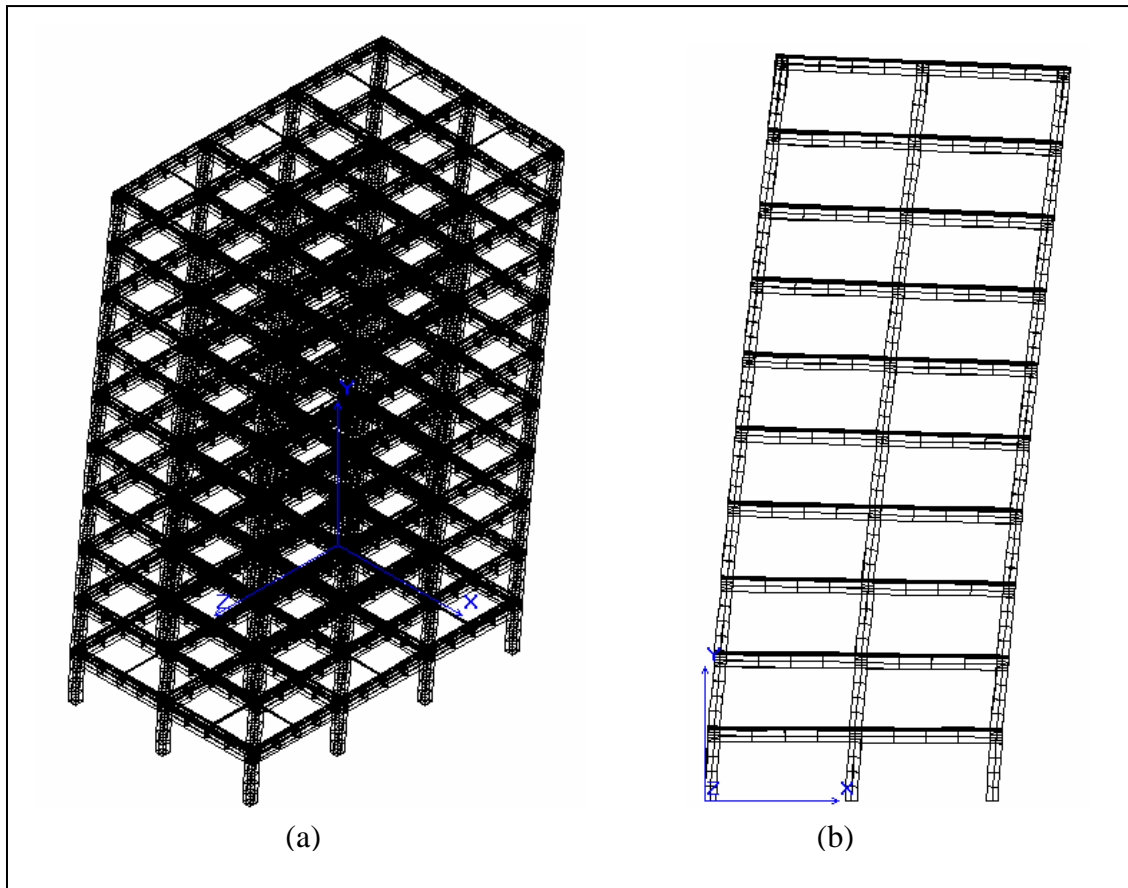


Figure 6.2: Deformed shape of frame structure; (a) 3D view and (b) Side view

6.2.2 Behaviour of Stress Analysis of the Frame Structure

Two types of material failures mainly cracking and crushing of concrete were observed in this study. Cracking is a material failure as a result of tension stress. In this study, cracking is assumed to occur in concrete elements when the maximum principal stress, P_1 of concrete exceeds $0.1f_{cu}$ i.e. 3.5 N/mm^2 . This is the limit of concrete tensile splitting or in other words concrete cracking.

The second mode of material failure is concrete crushing. In this study, if the minimum principal stress, P_3 of concrete is greater than $0.8f_{cu}$, i.e. 28N/mm^2 , the concrete element is assumed to have failed in crushing in the compression state.

6.2.2.1 Concrete Cracking

During the initial stages of applying the load, the frame structure exhibited no signs of distress and no visible cracking occurred. For the frame structure including the slabs, crack started to occur near the frame structure supports when the loading reached 346.6 kN at arc step 17 (Refer to Figure 6.1). At particular arc step 17, the nodes 241 (associated with element 99), 118 (element 49), 235 (element 97), 124 (element 51), 121 (element 51 and 49) and 238 (element 99 and 97) had reached the maximum principal stress of 3.59 N/mm^2 . Figure 6.3 illustrates the contour plot of P_1 at arc step 17. The initial cracking near the supports occurred when the maximum deflection at the top of the frame structure is 11.03 mm at node 19789 (Refer to Figure 6.4).

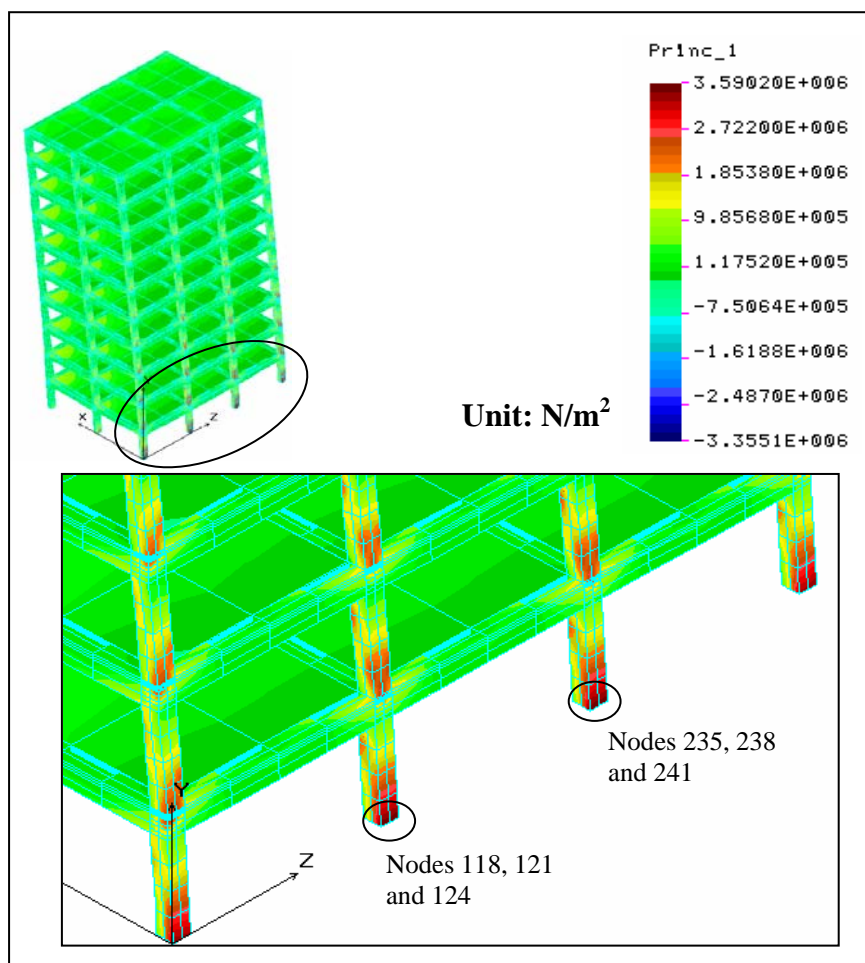


Figure 6.3: Contour plot of maximum principal stress, P_1 , at arc step 17

For the frame structure model without slabs, crack started to occur near the frame structure supports that is when the loading reached 353.6 kN at arc step 19 (Refer to Figure 6.1). At particular arc step 19, the nodes 241 (element 99), 118 (element 49), 235 (element 97), 124 (element 51), 121 (element 51 and 49), 1 (element 1), 358 (element 147), 355 (element 145 and 147), 4 (element 1 and 3) and 238 (element 99 and 97) had reached the maximum principal stress of 3.66 N/mm^2 . Figure 6.5 illustrates the contour plot of P_1 at arc step 19. The corresponding maximum deflection when the initial cracking occurred at the supports is 13.34 mm. The maximum deflection is observed at node 18757 (refer to Figure 6.6).

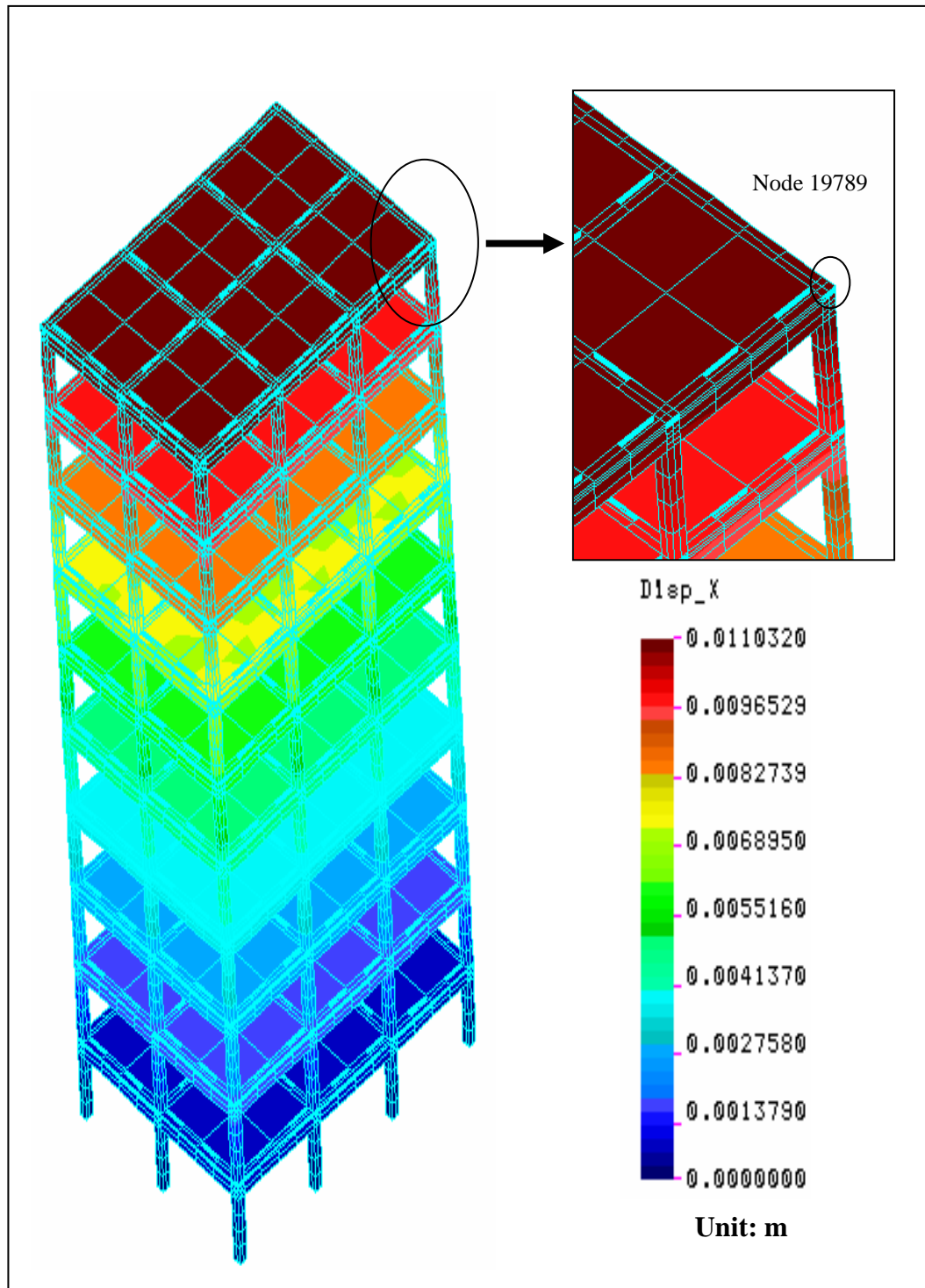


Figure 6.4: Contour plot of deflection at arc step 17

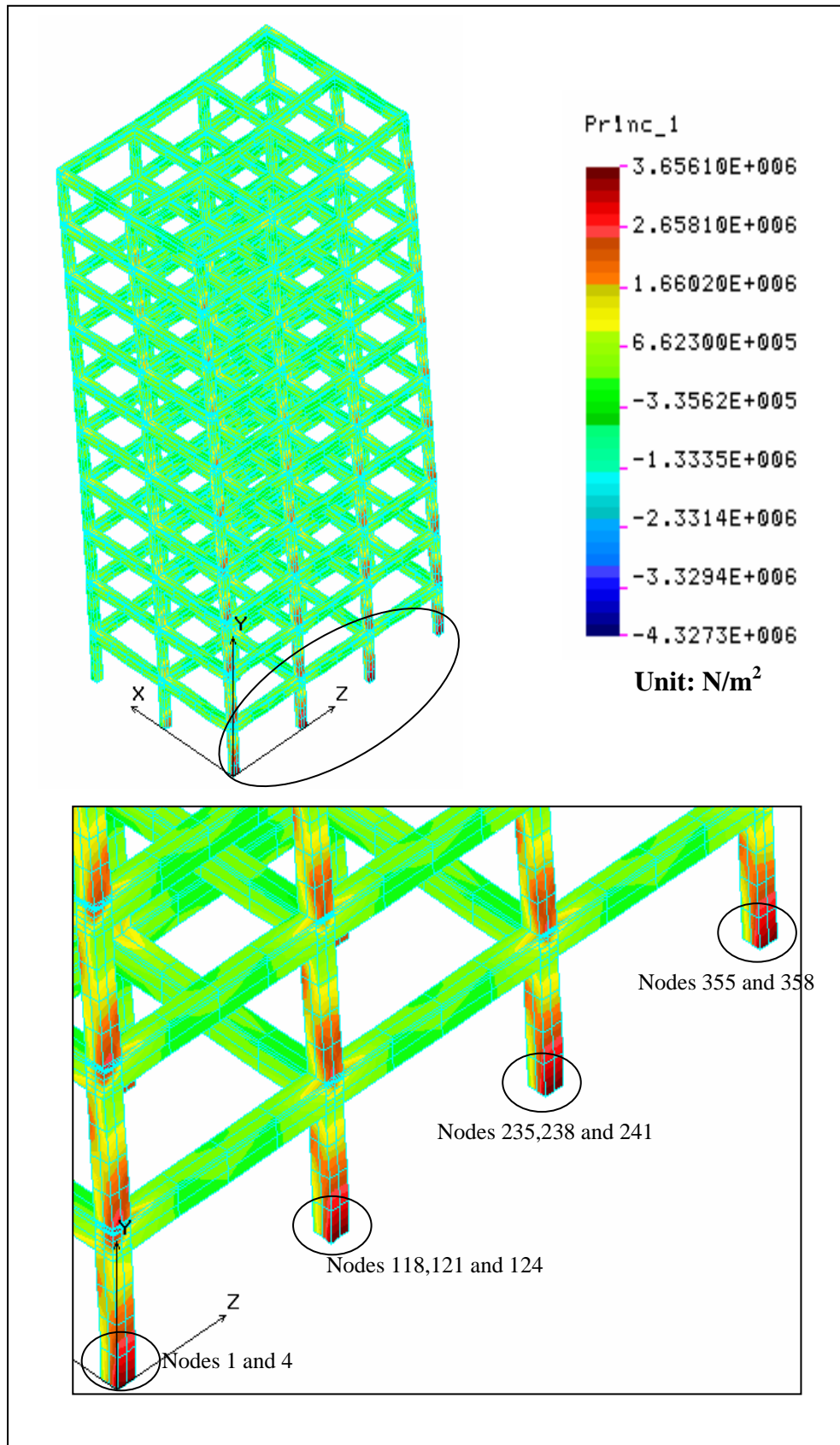


Figure 6.5: Contour plot of maximum principal stress, P_1 , at arc step 19

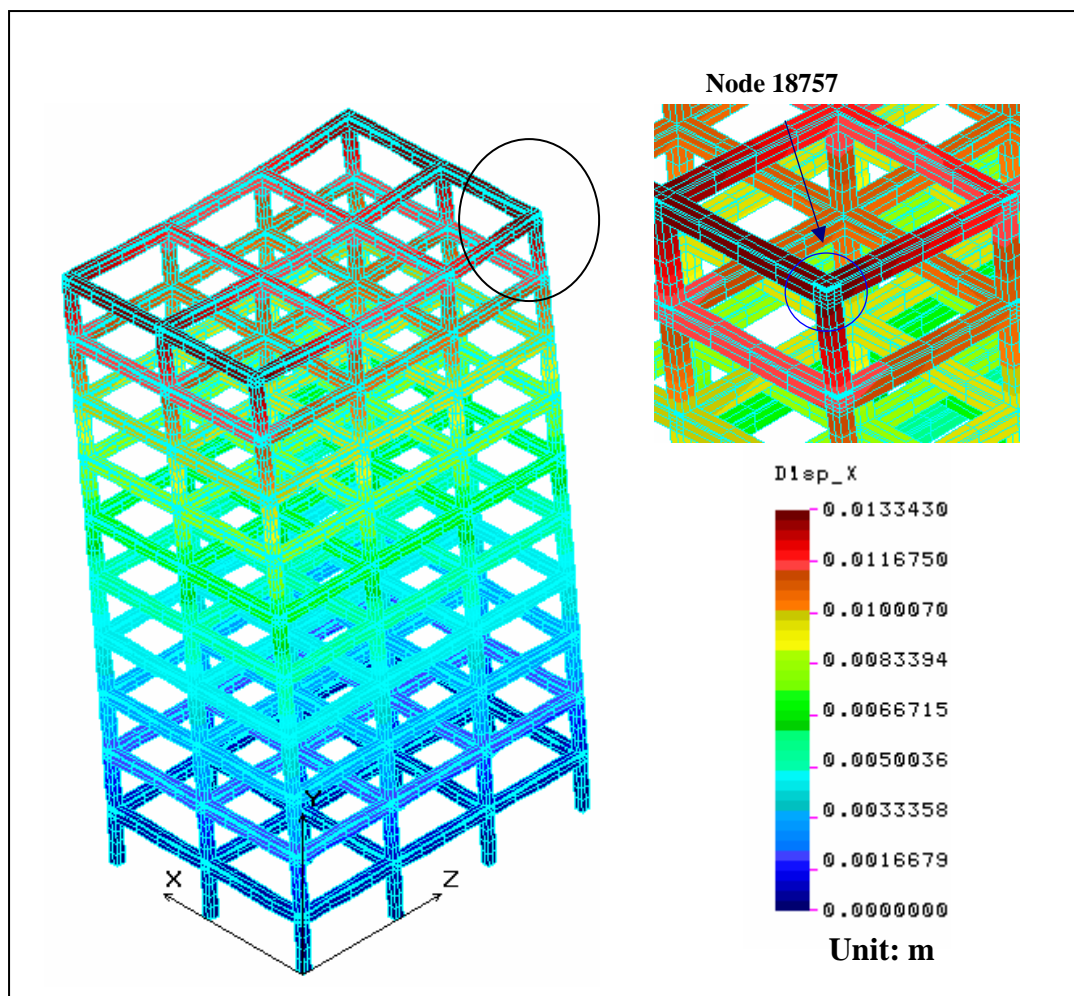


Figure 6.6: Contour plot of deflection at arc step 19

6.2.2.2 Concrete Crushing

For the frame structure model with slabs, concrete crushed at arc step 77 with the ultimate loading of 1419.9 kN. Concrete crushing occurred at node 19735 (element 11115) and node 19405 (element 10969). The locations of node 19735 and node 19405 are near the point load at the highest columns. The minimum principal stress recorded at those nodes is -28.75 N/mm^2 which exceeds the allowable compression stress of $0.8f_{cu}$ (-28 N/mm^2). The contour plot of minimum principal stress for the full model is as illustrated in Figure 6.7.

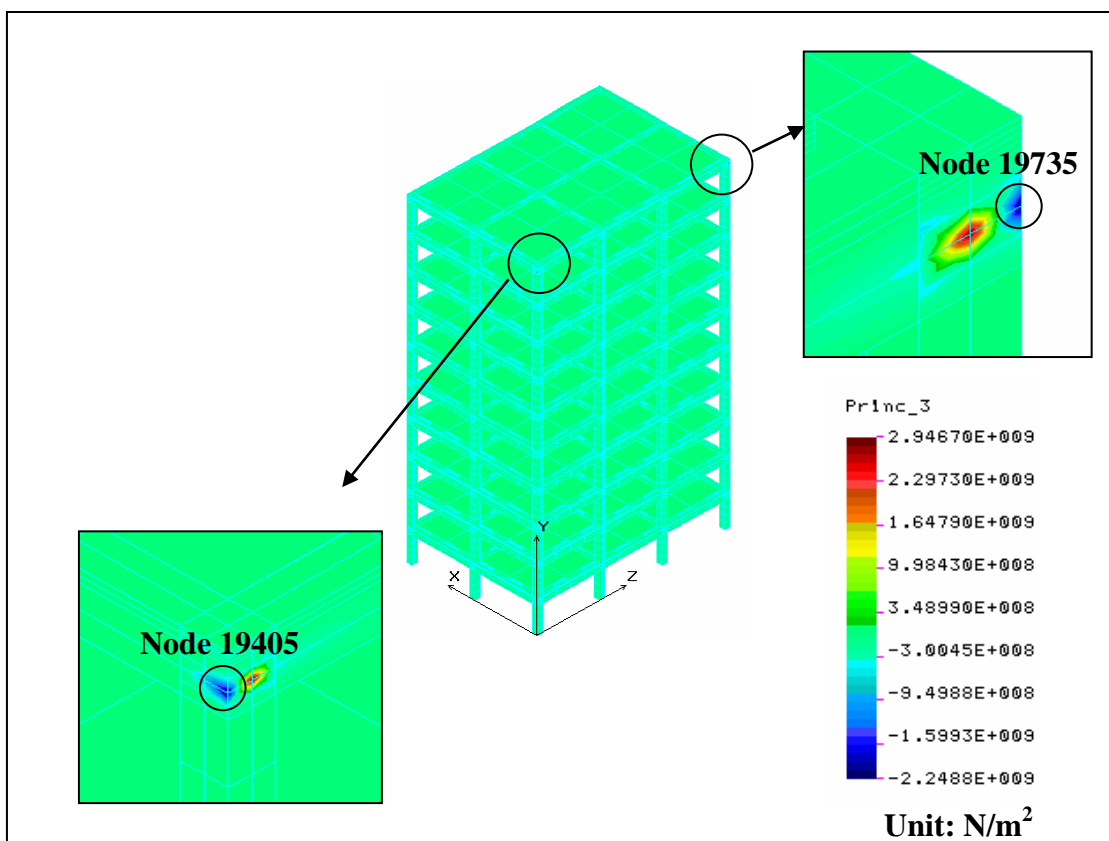


Figure 6.7: Contour plot of the minimum principal stress, P_3 , of the frame structure model which include slabs (Arc step 77)

Figure 6.8 illustrates the contour plot of the minimum principal stress, P_3 , for the frame without slabs. At arc step 83, concrete crushing occurred at node 18707 (element 10108) and node 19031 (element 10245) which are located at the most top of the columns. The minimum principal stress recorded at these nodes is -30.06 N/mm^2 which exceeds the allowable compression stress of $0.8f_{cu}$ (-28 N/mm^2). It is observed that, the ultimate loading at current step is 1396.35 kN.

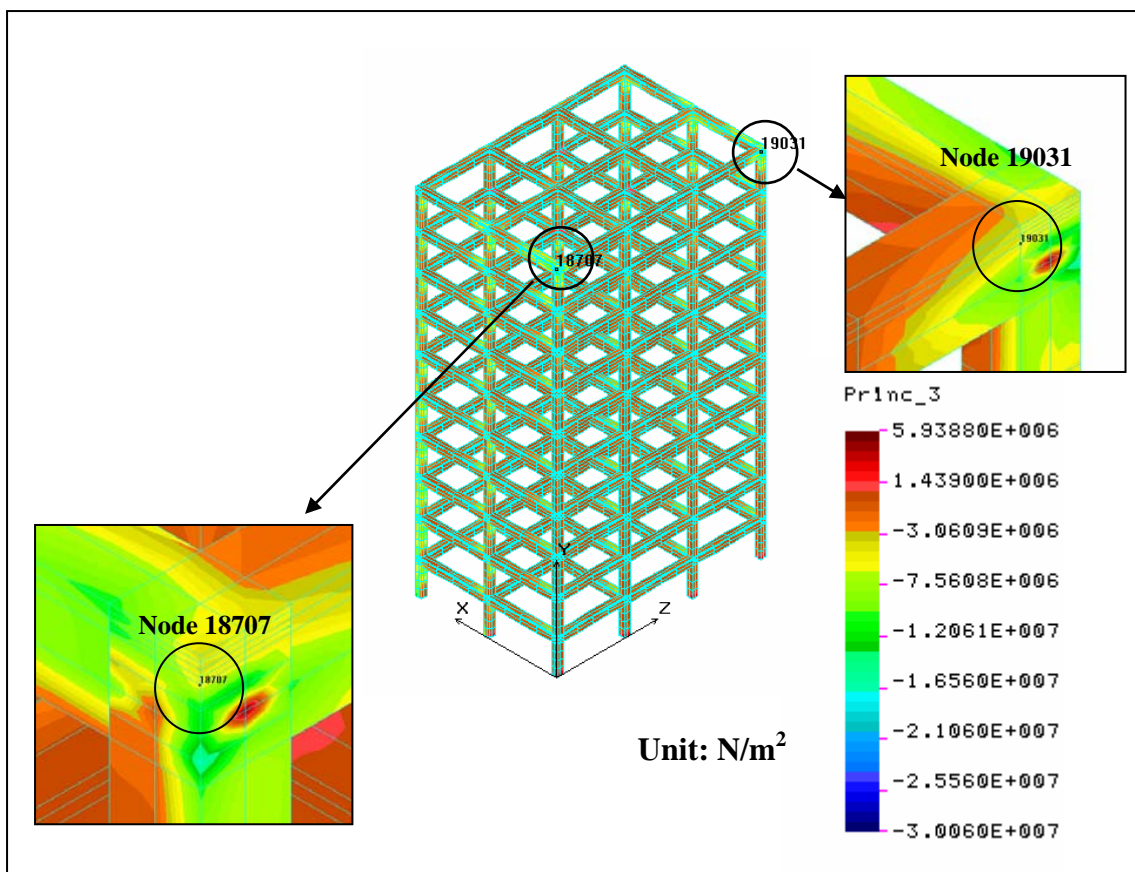


Figure 6.8: Contour plot of the minimum principal stress, P_3 , of the frame structure model which excluding slabs (Arc step 83)

6.3 Conclusion

The load-deflection curve shown in Figure 6.1 indicates the location of concrete cracking and crushing at the associated load. For the frame model with slabs, the concrete failed by cracking at arc step 17 and failed by crushing at arc step 77. Figure 6.1 also indicates the cracking point (arc step 19) and crushing point (arc step 83) for the frame model without slabs.

By comparing the deflection of the two models with the load of 400kN, 800kN and 1200kN, the slabs have increased the lateral stability of the frame structure by 16% to 18% as compared to the frame without slabs.

CHAPTER 7

CONCLUSIONS AND RECOMMENDATIONS

7.1 Introduction

The proposed frame structure has been successfully modelled using a nonlinear finite element approach. Concrete cracking will occur if the maximum principal stress, P_1 exceeds 10% of the tensile strength of concrete whereas concrete crushing will only occur if the minimum principal stress, P_3 , exceeds 80% of the compressive strength of concrete.

7.2 Conclusions

Based on the limited studies, the following conclusions are highlighted:-

- 1) It is seen from this study, that the analysis of slabs subjected to lateral force can be modelled as a strut and tie.

- 2) Cracking for the frame model with slabs observed in this study is at 10.3% of the tensile strength of the concrete and cracking for the frame model without slabs is at 10.5% of the tensile strength of the concrete, which are exceed the 10% of tensile strength as described in the theory.
- 3) From this study, crushing for the frame model with slabs is at 82.14% of the compressive strength of concrete and crushing for the frame model without slabs is at 86% of the compressive strength of concrete, which are exceed the 80% of compressive strength as describe in the theory.
- 4) The slabs are observed to act as a deep beam in transmitting horizontal loads from the slabs to the columns. Thus, the floor slabs play important role in transferring the horizontal loads to the lateral resisting system, i.e. the columns.
- 5) In terms of deflection response, this is clearly showed in the load-deflection response. The frames without slabs have larger deflections as compared to frames with slabs.
- 6) As can be seen from the study, the slabs can increase the lateral stability of bare frames by about 16% to 18%.

7.3 Recommendations for Future Research Work

Several recommendations are proposed for future studies of the effects of floor slabs in multi-storey frames.

The recommendations are as follows:

- Study may be conducted on other common thicknesses of floor slab in multi-storey frames such as 150mm and 200mm. Besides that, other common dimensions for beams and columns in multi-storey frames may also be carried out.
- Re-analyse the frame structure by using smaller element meshing so that the higher percentage of accuracy of stresses of the NLFEA results can be achieved.
- Re-analyse the frame structure with different grade of concrete, f_{cu} .

REFERENCES

- British Standards Institution (1984). *BS 6399: British Standard Codes of Practice for Dead and Imposed Loads*. London.
- British Standards Institution (1985). *BS 8110: British Standard Codes of Practice for Design and Construction*. London.
- Fernandes, G.R., and Venturini, W.S., (2002). *Non-Linear Boundary Element Analysis of Plates Applied to Concrete Slabs. Engineering Analysis With Boundary Elements. Volume 26*. 2002. pg 169-181.
- Bungale S. Taranath., (1988). *Steel, Concrete, and Composite Design of Tall Buildings*. McGraw-Hill.
- Lee DG, Kim HS., (2002). An efficient element for analysis of frames with shear walls. *ICES88, 1988 Apr*; Atlanta.
- Weaver W Jr, Johnson PR., (1987). *Structural dynamics by finite elements*. Prentice Hall, 1987.
- Bryan Stafford Smith., (1991). *Tall Building Structures: Analysis and Design*. New York: Wiley-Interscience.
- S. H. Ju. (2000). Comparison of building analyses assuming rigid or flexible floors-Closure. *Journal of Structural Engineering ASCE. Vol. 126*, 2000, pp. 273-274.

- Nakashima N., Huang T., Lu L. W. Effect of diaphragm flexibility on seismic response of building structures. *Proc. 8th WCEE*, Vol. 4, 735-742.
- Dong-Guen Lee and Hyun-Soo Kim. (2000). The Effect of Floor Slabs on the Seismic Response of Multi-Story Building Structures. *Proceedings of 4th APSEC, 13-15 September 2000 Kuala Lumpur, Malaysia*. **Vol.1**, pg 453-461.
- Kotsovos, M.D. and Pavlovic, M.N. (1995). *Structural Concrete: Finite-Element Analysis for Limit-State Design*. London: Thomas Telford.
- Marsono A.K. (2000). *Reinforced Concrete Shear Wall With Regular Staggered Openings*. University of Dundee: Ph.D. Thesis, **Volume 1**.
- Marsono A.K., and Subedi N.K. (2000). Analysis of Reinforced Concrete Shear Wall Structures With Staggered Openings, Part II: Non-linear Finite Element Analysis (NLFEA). *Proceeding of the 4th Asian-Pacific Structural Engineering and Construction Conference (APSEC2000)*. September 13th-15th, 2000. Kuala Lumpur. Pg 341-355.
- Shanmugam, N.E., Kumr, G., and Thevendran, T. (2002). Finite Element Modelling of Double Skin Composite Slabs. *Finite Element in Analysis and Design*. **Volume 38**. 2002. pg 579-599.
- Structural Research and Analysis Corporation (SRAC) (1992). *Introduction to COSMOS/M PC Version*. Fifth Edition. California.
- Yam, Lloyd, C.P. (1981). *Design of Composite Steel-Concrete Structures*. London: Surrey University Press.
- Bathe, K.J. (1982). *Finite Element Procedures in Engineering Analysis*. Englewood Cliffs, New Jersey: Prentice-Hall, Inc.
- Bedard, C. and Kotsovos, M.D. (1985). Application on NLFEA to Concrete Structures. *Journal of Structural Engineering*. 111: 2691-2707.

Carlton, D (1993). Application of the Finite Element Method to Structural Engineering Problems. *The Structural Engineer*. 71: 55-59.

Weaver, W.J. and Johnston, P.R. (1984). *Finite Element for Structural Analysis*. Englewood Cliffs, New Jersey: Prentice-Hall, Inc.

APPENDIX A

Stress-Strain Data for Concrete in Compression

Reference: BS 8110, Part II

Concrete characteristic strength, f_{cu}	:	0.8 x 35 = 28 N/mm ²
Concrete compressive tangent modulus, E_c	:	21.7 N/mm ²
Concrete compressive start of plastic, f_c'	:	6.66 N/mm ²
Concrete compressive peak strength	:	0.0022 N/mm ²
Concrete compressive ultimate strength	:	0.0035 N/mm ²

$$\text{Stress, } \sigma = 0.8f_{cu} \left(\frac{k\eta - \eta^2}{1 + (k-2)\eta} \right)$$

$$\eta = \frac{\varepsilon}{\varepsilon_{c,1}}$$

$$= \frac{\varepsilon}{0.0022}$$

$$k = \frac{1.4\varepsilon_{c,1}E_o}{f_{cu}}$$

$$= \frac{3E_o}{f_{cu}}$$

Note: σ is the stress in concrete

E_o is the modulus elasticity of concrete in kN/mm² 615 the strain in concrete

ε is the strain in concrete

$\varepsilon_{c,1}$ is the strain in concrete at the maximum stress

Calculated stress-strain value for concrete in compression:

<u>Strain (m/m)</u>	<u>Stress (N/m²)</u>
0	0
0.0001	2859004.377
0.0002	5523580.173
0.0003	8001978.435
0.0004	10301989.86
0.0005	12430976.43
0.0006	14395900.55
0.0007	16203351.75
0.0008	17859571.32
0.0009	19370475.06
0.001	20741674.17
0.0011	21978494.62
0.0012	23085995.09
0.0013	24068983.45
0.0014	24932032.19
0.0015	25679492.6
0.0016	26315508.02
0.0017	26844026.09
0.0018	27268810.18
0.0019	27593450.03
0.002	27821371.61
0.0021	27955846.41
0.0022	28000000
0.0023	27956820.11
0.0024	27829164.12
0.0025	27619766.13
0.0026	27331243.47
0.0027	26966102.95
0.0028	26526746.57
0.0029	26015476.97
0.003	25434502.51
0.0031	24785942.04
0.0032	24071829.41
0.0033	23294117.65
0.0034	22454682.99
0.0035	21555328.57
0.00351	15000000
0.00352	6000000
0.00353	0

APPENDIX B**Ses File for Frame Model in COSMOS/M**

PT,1,0,0,0
PT,2,0.5,0,0
PT,3,0.5,0,0.5
PT,4,0,0,0.5
SF4PT,1,1,2,3,4,0
SFGEN,1,1,1,1,0,0,2.5,0
VL2SF,1,1,2,1
SFGEN,1,2,2,1,0,0,0.5,0
VL2SF,2,2,7,1
SFGEN,1,7,7,1,0,0,0.135,0
VL2SF,3,7,12,1
VLGEN,3,1,3,1,0,0,0,6
VLGEN,2,1,12,1,0,6,0,0
VL2SF,37,10,38,1
VL2SF,38,15,53,1
VLGEN,2,37,38,1,0,0,0,6
VLGEN,2,37,42,1,0,6,0,0
VL2SF,55,11,80,1
VL2SF,56,16,90,1
VLGEN,1,55,56,1,0,6,0,0
VLGEN,3,55,58,1,0,0,0,6
VL4SF,71,199,262,222,282,1
VLGEN,1,71,71,1,0,6,0,0
VLGEN,2,71,72,1,0,0,0,6
EGROUP,1,SOLID,0,2,0,0,4,0,0,0
MPROP,1,DENS,2400
MPROP,1,EX,2.17E10
MPROP,1,NUXY,0.2
MPROP,1,SIGYLD,15.63E6
MPROP,1,EY,2.17E10
MPROP,1,EZ,2.17E10

MPROP,1,NUXZ,0.2
MPROP,1,NUYZ,0.2
RCONST,1,1,1,9,0,0,0,0,0,0,0
VLGEN,9,1,76,1,0,0,3.135,0
MPC,1,0,1,-0.00353,0,-0.00352,-6000000,-0.00351,-15000000,-0.00350,-23&
574261,-0.00340,-24169048,-0.00330,-24728972,-0.00320,-25252316,-0.003&
10,-25737250,-0.00300,-26181818,-0.00290,-26583932
MPC,1,0,11,-0.00280,-26941354,-0.00270,-27251689,-0.00260,-27512365,-0&
.00250,-27720621,-0.00240,-27873486,-0.00230,-27967763,-0.00220,-28000&
000,-0.00210,-27966472,-0.00200,-27863148,-0.00190,-27685660
MPC,1,0,21,-0.00180,-27429270,-0.00170,-27088826,-0.00160,-26658718,-0&
.00150,-26132825,-0.00140,-25504456,-0.00130,-24766283,-0.00120,-23910&
259,-0.00110,-22927536,-0.00100,-21808354,-0.00090,-20541924
MPC,1,0,31,-0.00080,-19116291,-0.00070,-17518169,-0.00060,-15732749,-0&
.00050,-13743481,-0.00040,-11531804,-0.00030,-9076831,-0.00020,-635497&
8,-0.00010,-3339511,0.00000,0,0.000129,2800000,0.003,0
MPCTYP,1,0
ACTSET,EG,1
ACTSET,MP,1
ACTSET,RC,1
ACTSET,MC,1
M_VL,1,760,1,8,2,2,4,1,1,1
NMERGE,1,34200,1,0.0001,0,1,0
NCOMPRESS,1,34196
DSF,1,AL,0,1,1
DSF,17,AL,0,19,1
DSF,65,AL,0,65,1
DSF,97,AL,0,97,1
DSF,129,AL,0,129,1
DSF,161,AL,0,161,1
DSF,66,AL,0,66,1
DSF,98,AL,0,98,1
DSF,130,AL,0,130,1
DSF,162,AL,0,162,1
FND,19408,FX,50000,19408,1
FND,19732,FX,50000,19732,1
NL_CONTROL,2,0,1E+008,0.035,100,5,1,0,0.5
NL_AUTOSTEP,1,1E-008,0.035,5
A_NONLINEAR,S,1,1,20,0.01,0,N,0,0,1E+010,0.001,0.01,0,1,0